Environmental Science & Technology

Article

pubs.acs.org/est

Responses of the Proteome and Metabolome in Livers of Zebrafish Exposed Chronically to Environmentally Relevant Concentrations of Microcystin-LR

Liang Chen,[†,‡,#] Yufei Hu,[†,‡,#] Jun He,[†] Jun Chen,[*,†] John P. Giesy,[§,∥,⊥] and Ping Xie[*,†]

[†]Donghu Experimental Station of Lake Ecosystems, State Key Laboratory of Freshwater Ecology and Biotechnology, Institute of Hydrobiology, Chinese Academy of Sciences, Wuhan 430072, China

[‡]University of Chinese Academy of Sciences, Beijing 100049, China

[§]Department of Veterinary Biomedical Sciences and Toxicology Centre, University of Saskatchewan, Saskatoon, Saskatchewan S7N 5B3, Canada

[∥]School of Biological Sciences, University of Hong Kong, Hong Kong SAR, China

[⊥]State Key Laboratory of Pollution Control and Resource Reuse, School of the Environment, Nanjing University, Nanjing, 210089, China

Supporting Information

ABSTRACT: In this study, for the first time, changes in expressions of proteins and profiles of metabolites in liver of the small, freshwater fish Danio rerio (zebrafish) were investigated after long-term exposure to environmentally relevant concentrations of microcystin-LR (MC-LR). Male zebrafish were exposed via water to 1 or 10 μg MC-LR/L for 90 days, and iTRAQ-based proteomics and ^{1}H NMR-based metabolomics were employed. Histopathological observations showed that MC-LR caused damage to liver, and the effects were more pronounced in fish exposed to 10 μg MC-LR/L. Metabolomic analysis also showed alterations of hepatic function, which included changes in a number of metabolic pathways, including small molecules involved in energy, glucose, lipids, and amino acids metabolism. Concentrations of lactate were significantly greater in individuals exposed to MC-LR than in unexposed controls. This indicated a shift toward anaerobic metabolism, which was confirmed by impaired respiration in mitochondria. Proteomics revealed that MC-LR significantly influenced multiple proteins, including those involved in folding of proteins and metabolism. Endoplasmic reticulum stress contributed to disturbance of metabolism of lipids in liver of zebrafish exposed to MC-LR. Identification of proteins and metabolites in liver of zebrafish responsive to MC-LR provides insights into mechanisms of chronic toxicity of MCs.

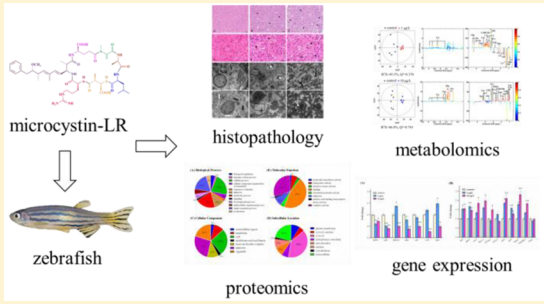

INTRODUCTION

Due to a combination of factors including eutrophication and warming, blooms of cyanobacteria and associated releases of cyanotoxins as extracellular products, are increasing worldwide.[1,2] Microcystins (MCs), a group of monocyclic heptapeptides (molecular weight about 1000 Da), are the most frequently reported cyanobacterial toxins and are regarded as a major hazard to health of humans and present challenges to quality of drinking water.[3−6] More than 100 MCs have been identified. Although variations have been reported among all of the amino acids, substitutions of the variable L-amino acids X and Z in positions two and four are most prevalent[7,8] MC-LR is one of the most common and potent variants, which is why it has been the most widely studied. In most cases, concentrations of dissolved MCs in water are relatively small, within a range of 0.1−10 μg/L, whereas cell-bound concentrations are several orders of magnitude greater.[9−12] MCs are of concern due to their adverse effects, such as hepatotoxicity, carcinogenicity, reproductive toxicity, neurotoxicity, immunotoxicity, and endocrine-disrupting effects.[13,14] Exposure of humans to MCs can occur via ingestion of contaminated drinking water and/or consumption of cultivated plants, aquatic products including fish and blue-green algae supplements (BGAS).[13,15] In 1998, the World Health Organization (WHO) established a provisional guideline value of 1 μg MC-LR/L in drinking water.[15,16] In 2010, the International Agency for Research on Cancer (IARC) classified MC-LR as being "possibly carcinogenic to humans" (Group 2B carcinogen).[17]

Compared to terrestrial organisms, aquatic organisms (including fishes) are more frequently exposed to MCs. Since MCs are released from cyanobacterial cells into waters, the first

Received: August 8, 2016
Revised: November 29, 2016
Accepted: December 5, 2016
Published: December 5, 2016

DOI: 10.1021/acs.est.6b03990
Environ. Sci. Technol. 2017, 51, 596−607

contact point for MCs would be through the aquatic environment.[18] Most aquatic organisms can come into contact with MCs, or with cyanobacterial cells, with subsequent accumulation of MCs in the aquatic food web.[19−22] Similar to mammals, results of both field and laboratory studies have demonstrated that the liver is the primary target organ for MCs and studies on various fishes have shown that MCs accumulate mainly in liver, but also in gill, brain, intestine, and viscera.[18,21,23] MCs can affect biochemical, histopathological, and behavioral patterns, osmoregulation, and growth, development, and reproduction.[23]

Magnitudes of toxic effects, induced by MCs, depend on route and magnitude of exposure to the toxin. Primary routes of exposure used to assess effects of MCs on fish include intraperitoneal (i.p.) injection, oral gavage, dietary and immersion in water containing purified MCs, lysates, crude extracts or whole cells of cyanobacteria.[23] Several studies of MCs have used i.p. injection or oral exposure, but few studies have studied effects of water-borne exposures of fishes.[18,24,25] MCs are less potent when exposed to contaminated water than when they are injected intraperitoneally (i.p.).[23,26] Therefore, to obtain information that is more appropriate for predicting potential for adverse effects under field conditions, waterborne exposure is more relevant. Most studies of MCs, results of which are in the literature, focused on acute and subchronic toxicities of MCs, while fewer efforts have been devoted to explore chronic effects of MCs.[22,27−30] In aquatic ecosystems, chronic exposure to MCs is the main pathway of exposure of aquatic organisms to MCs. Concentrations of MCs are often a few μg/L in waters of eutrophic lakes around the world. Also, due to chemical stabilities and resistances of MCs to breakdown, organisms can be exposed to lesser concentrations of MCs, but for longer periods following lyses of the bloom. Therefore, in order to make realistic evaluations of toxicity of MCs to fish, longer-term chronic exposure by immersion needed to be studied.[18,22]

Zebrafish (*Danio rerio*), a small, tropical, freshwater fish, represents an important vertebrate model organism that is widely used in toxicological research because they are small, available in large numbers, and easily maintained under laboratory conditions at small husbandry costs. With the emergence of system biology, the "-omic" approaches, such as transcriptomics, proteomics and metabolomics, are capable of discovering broader ranges of biomarkers at molecular levels and are increasingly being employed to investigate mechanisms of toxic action of contaminants. Use of zebrafish is effective since the genome of this species is known and annotated.[31]

To our knowledge, previously there have been no studies combining proteomics and metabolomics for study of effects of MCs on any aquatic organism or investigations of toxicological effects of chronic exposure of aquatic organisms to MCs. In the study, results of which are presented here, a complementary pathological, proteomic and metabolomic approach was used to elucidate responses of zebrafish to environmentally relevant concentrations of MC-LR. To further investigate some of the molecular pathways modulated by MCs, expressions of mRNA for selected genes, identified by use of the omics approaches, were measured by use of quantitative real-time polymerase chain reactions (qRT-PCR).

MATERIALS AND METHODS

Zebrafish and Exposure to MC-LR. Healthy, adult, male zebrafish (AB strain), about 3 months old, were obtained from the China Zebrafish Resource Center, Institute of Hydrobiology, Chinese Academy of Sciences. Zebrafish were randomly divided into 20 L glass tanks containing 12 L charcoal-filtered tap water (20 fish per tank) and acclimated for 2 weeks prior to exposure to MCs. Temperature was maintained at 28 ± 0.5 °C with a 12:12 light/dark cycle and zebrafish were fed with freshly hatched brine shrimp twice daily and flake food once daily. Purified MC-LR (purity ≥95%) was purchased from Taiwan Algal Science Inc. (China). After acclimation, three replicate tanks were randomly assigned to each exposure group, and zebrafish were exposed to 0, 1, or 10 μg/L for 90 days. The range of exposure concentrations was based on previous studies.[22,32,33] One-third of water of the appropriate concentration of MC-LR was replaced by fresh water every 3 days. After 90 days of exposure, zebrafish were anesthetized in ice-cold water and livers were collected. One portion was placed in Bouin's solution or 2.5% glutaraldehyde, and the remaining livers were immediately frozen in liquid nitrogen and stored at −80 °C until analysis. All procedures carried out on fish were approved by the Institutional Animal Care and Use Committee (IACUC), and were in accordance with the National Institutes of Health Guide for the Care and Use of Laboratory.

ELISA Detection of Concentrations of MC-LR in Water. Before and during the exposure, concentrations of MC-LR were monitored after replenishment of water. A sample of 1 mL of water was collected from each tank and stored at −20 °C until analysis. Concentrations of MC-LR were determined by using the commercially available microcystin plate kit (Beacon Analytical Systems, Inc., Saco) with comparison to external standards. The minimum detection limit (MDL) for MCs is 0.1 μg/L.

Light and Electron Microscopy. Histopathological analyses were conducted by use of previously described methods.[34] Briefly, for light microscopy, livers were fixed in Bouin's solution and embedded in paraffin and blocks were sectioned on a microtome. The 5 μm thick liver sections were stained with hematoxylin and eosin (H&E). Histological observation was performed using light microscopy.

For transmission electron microscopy (TEM), liver tissue was diced into 1 mm^3, prefixed in 2.5% glutaraldehyde solution and fixed in 1% aqueous osmium tetroxide. The specimens were then embedded in Epon 812. Ultrathin sections were sliced with glass knives on a LKB-V ultramicrotome (Nova, Sweden), stained with uranyl acetate and lead citrate and examined by Tecnai G2 20 TWIN (FEI).

iTRAQ-Based Quantitative Proteomic Analysis. Quantitative proteomic analysis was performed according to the methodology described in previous studies,[25,35,36] with some modifications, of which details are given in the Supporting Information (SI). Briefly, livers from 5 individuals of each tank were pooled as one replicate (n = 2), and proteins were extracted by use of trichloroacetic acid/acetone. Concentrations of protein in extracts were determined by use of a 2-D Quant kit (GE Healthcare, Pittsburgh, PA). Subsequently, 100 μg protein for each sample was reduced with dithiothreitol, alkylated with iodoacetamide, digested with sequence-grade modified trypsin, and labeled with iTRAQ (isobaric tag for relative and absolute quantitation) reagents (AB Sciex, Foster City, CA). Pooled peptides were cleaned-up, desalted, and then separated using high pH reverse-phase high-performance liquid chromatography (HPLC) using an Agilent 300 Extend C18 column (Santa Clara, CA). Fractionated samples were analyzed

DOI: 10.1021/acs.est.6b03990
Environ. Sci. Technol. 2017, 51, 596−607

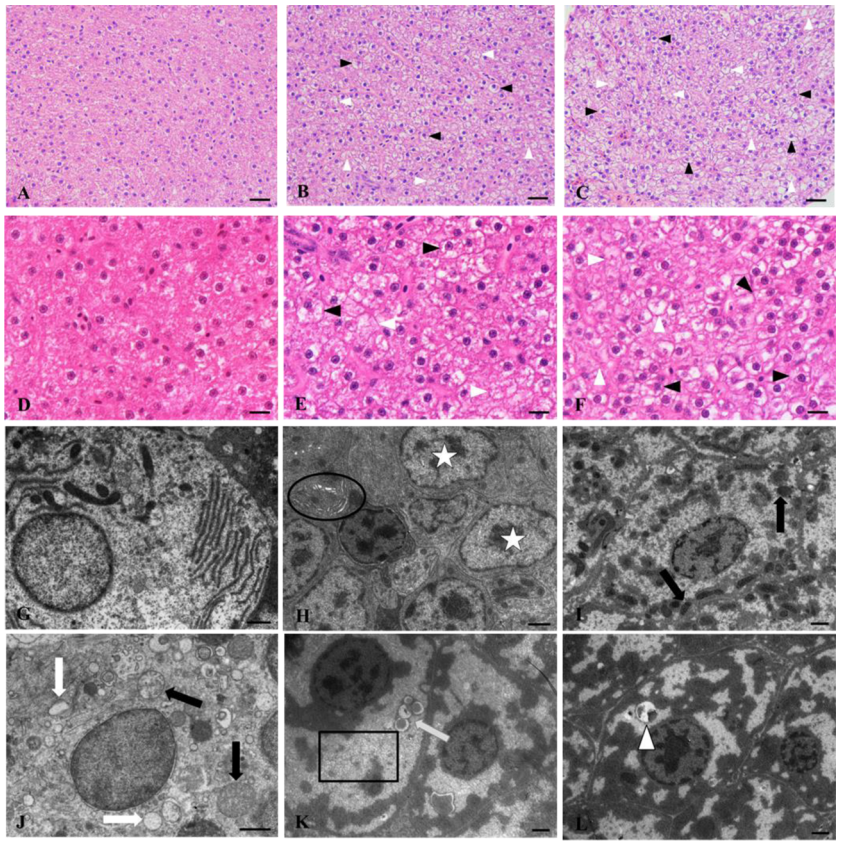

Figure 1. Micro- and ultrastructural changes in liver of zebrafish exposed to 1 or 10 μg MC-LR/L for 90 days. (A) (D) Control group. (B) (E) 1 μg MC-LR/L, showing swollen hepatocytes (black arrowhead), and cell vacuolar degeneration (white arrowhead). (C) (F) 10 μg MC-LR/L, showing swollen hepatocytes (black arrowhead), and cell vacuolar degeneration (white arrowhead). (G) Control group. (H) 1 μg MC-LR/L, showing cell shrinkage (white star), and dilation of rough endoplasmic reticulum (black circle). (I) 1 μg MC-LR/L, showing swollen mitochondria (black arrow). (J) 10 μg MC-LR/L, showing vacuoles (white arrow), and swollen mitochondria (black arrow). (K) 10 μg MC-LR/L, showing hyperplasia of smooth endoplasmic reticulum associated with mild expansion (black box), and lysosomes (gray arrow). (L) 10 μg MC-LR/L, showing autophagic vacuole (white arrowhead). (A) (B) (C), bar = 25 μm, (D) (E) (F), bar = 10 μm, (G) (H) (I) (J) (K) (L), bar = 1 μm.

by use of a Q Exactive Plus hybrid quadrupole-Orbitrap mass spectrometer (ThermoFisher Scientific, Waltham, MA). Proteins with $p < 0.05$ and fold difference >1.2 or <0.83 were considered differentially expressed. Functions of differentially expressed proteins were were determined by use of Gene Ontology (GO) annotation, Kyoto Encyclopedia of Genes and Genomes (KEGG) pathway analysis, and functional enrichment analysis. The GO classification was done using UniProt-GOA database (http://www.ebi.ac.uk/GOA/) and InterProScan soft. Wolfpsort was used to predict subcellular localization of the proteins.

For quality control purposes, mass errors and lengths of all peptides were analyzed. The distribution of mass error was near zero and mostly less than 0.02 Da (SI Figure S1A), which means the mass accuracy of the MS data was sufficient. Also, lengths of most peptides were distributed between 8 and 16 (SI Figure S1B), which agree with properties of tryptic peptides, so that the results met the standard.

HR-MAS ^{1}H NMR-Based Metabolomic Analysis. Metabolites in liver were analyzed by use of a Bruke Avance 600 NMR spectrometer (Bruker Biospin, Germany) equipped with a triple-field resonance (^{1}H/^{13}C/^{31}P) high resolution magic-angle-spinning (HR-MAS) probe as described previously,[37] with some modifications. More details about metabolomic analysis are given in the SI. Briefly, tissue samples were analyzed by HR-MAS ^{1}H NMR using a water-suppressed one-dimensional Carr−Purcell−Meiboom−Gill (CPMG) spin−echo pulse sequence (recycle delay −90°-(τ-180°-τ)$_n$- acquisition), with one liver as one replicate ($n = 6$). Nuclear magnetic resonance (NMR) spectra were Fourier transformed and corrected for phase and baseline shifts by use of MestReNova (version 7.0, Mestrelab Research, Spain). All spectra were referenced to the internal lactate CH_3 resonance at 1.33 ppm. Multivariate statistical analyses, including unsupervised principal component analysis (PCA), and supervised partial least squares discriminant analysis (PLS-DA) and orthogonal projection to latent structure with discriminant analysis (OPLS-DA) methods were performed by SIMCA-P+ (V11.0, Umetrics, Umea, Sweden). Correlation coefficients (|r|) > 0.755, which was determined according to the test for the significance of the Pearson's product-moment correlation coefficient, were considered statistically significant based on the discrimination significance at the level of $p < 0.05$ and degrees of freedom =5.

Quantitative Real-Time PCR (qRT-PCR). Five livers from each tank were pooled together as one replicate ($n = 3$). Isolation, purification, and quantification of total RNA were performed by use of previously described methods.[38] First-strand cDNA synthesis was carried out with random hexamers and oligo-dT primers. Sequences of primers used in qRT-PCR were designed with Primer Premier 5.0 (Premier, Canada) (SI Table S1). Housekeeping genes, *gapdh* and *18S rRNA* were

DOI: 10.1021/acs.est.6b03990
Environ. Sci. Technol. 2017, 51, 596−607

Table 1. Differentially Expressed Proteins (with Functional Annotation) In Liver of Zebrafish Exposed to MC-LR

protein accession[a]	protein description	fold change[b] 1 μg/L	fold change[b] 10 μg/L	function category
Amino Acid Metabolism				
F1Q6E1	4-hydroxyphenylpyruvate dioxygenase	2.09 ± 0.25	2.18 ± 0.06*	tyrosine metabolism
Q6TGZ5	4-hydroxyphenylpyruvate dioxygenase	0.28 ± 0.00**	0.30 ± 0.02**	tyrosine metabolism
F1QHM8	methylthioribulose-1-phosphate dehydratase	0.98 ± 0.03	0.73 ± 0.03*	methionine metabolism
Q1RLT0	S-adenosylmethionine synthase	1.02 ± 0.02	0.72 ± 0.01**	methionine metabolism
Protein Metabolism				
A8E526	Rpl14 protein	1.52 ± 0.15	1.28 ± 0.04*	ribosome biogenesis and assembly; protein biosynthesis
P62084	40S ribosomal protein S7	1.30 ± 0.06	1.35 ± 003*	ribosome biogenesis and assembly; protein biosynthesis
Q6P5L3	60S ribosomal protein L19	1.85 ± 0.40	1.44 ± 0.03*	ribosome biogenesis and assembly; protein biosynthesis
Q6PBV6	H/ACA ribonucleoprotein complex subunit 2-like protein	1.40 ± 0.09*	1.12 ± 0.07	ribosome biogenesis and assembly; protein biosynthesis
F1Q5S9	probable signal peptidase complex subunit 2	1.18 ± 0.06	1.35 ± 0.06*	protein processing
Q6NWJ2	signal peptidase complex subunit 3 homologue (S. cerevisiae)	1.32 ± 0.14	1.45 ± 0.06*	protein processing
Q7T2E1	SEC13 homologue (S. cerevisiae)	1.14 ± 0.11	1.39 ± 0.09*	protein transport
Lipid Metabolism				
A3QK15	acetoacetyl-CoA synthetase	1.61 ± 0.66	0.69 ± 0.03*	Fatty acid metabolism
Q4 V8S5	Acbd7 protein	1.95 ± 0.19*	1.48 ± 0.15	atty-acyl-CoA binding
Q58EG2	Erlin-1	1.12 ± 0.01	1.33 ± 0.03*	lipid metabolism
Q6DRN8	Cdipt protein	0.97 ± 0.04	1.30 ± 0.06*	lipid metabolism
Q7T2J4	alcohol dehydrogenase 8b	0.90 ± 0.16	0.67 ± 0.05*	lipid metabolism
Q9I8L5	fatty acid-binding protein 10-A, liver basic	0.99 ± 0.11	0.82 ± 0.02*	Fatty acid transport
O42364	apolipoprotein Eb	0.89 ± 0.13	0.72 ± 0.01**	lipid transport; lipoprotein metabolism
Mitochondrial Energy Metabolism				
Q6AZA2	NADH dehydrogenase (Ubiquinone) flavoprotein 1	0.89 ± 0.03	0.69 ± 0.03*	electron transport chain
Q6IQM2	cytochrome c	0.85 ± 0.10	0.70 ± 0.04*	electron transport chain
Q9MIY7	cytochrome c oxidase subunit 2	1.21 ± 0.02*	1.05 ± 0.07	electron transport chain
Other Metabolism				
A2BHD8	beta-hexosaminidase	1.22 ± 0.03*	1.38 ± 0.16	beta-N-acetylhexosaminidase activity
F8W5B8	phosphorylase	0.79 ± 0.17	0.70 ± 0.03*	glycogen phosphorylase activity
Q0E671	cytidine monophosphate sialic acid synthetase 1	1.33 ± 0.07*	1.22 ± 0.09	nucleotidyltransferase activity
Q5CZW2	uridine phosphorylase	0.75 ± 0.08	0.76 ± 0.03*	nucleotide metabolism
Q7ZUN6	phosphoribosylaminoimidazole carboxylase, phosphoribosylaminoimidazole succinocarboxamide synthetase	1.08 ± 0.17	0.73 ± 0.02**	nucleotide metabolism
Q8UVG6	cellular retinol-binding protein type II	0.74 ± 0.15	0.54 ± 0.02**	vitamin A metabolism
Chromatin Assembly and Modification				
E7F4R5	histone deacetylase 8	0.82 ± 0.18	0.70 ± 0.02*	histone deacetylase activity
G1K2S9	histone H3	1.34 ± 0.11	1.59 ± 0.12*	chromatin assembly
Q1RLR9	histone H2A	1.58 ± 0.07*	1.68 ± 0.23	chromatin assembly
Q6NUW5	acidic leucine-rich nuclear phosphoprotein 32 family member E	1.38 ± 0.13	1.23 ± 0.04*	H2A.Z chaperone
Signal Transduction				
F1QT29	calcium uniporter protein, mitochondrial	0.82 ± 0.03*	1.00 ± 0.04	calcium uptake into mitochondria
Q1LWV8	phosphoinositide phospholipase C	0.82 ± 0.03*	0.82 ± 0.04	signal transducer activity
Q2L6L1	protein canopy-1	1.57 ± 0.33	1.52 ± 0.08*	fibroblast growth factor receptor signaling pathway
Q803G3	serine/threonine-protein phosphatase 2A catalytic subunit	0.82 ± 0.01*	0.98 ± 0.03	signal transduction
Immune Response				
C1IHU8	intelectin 1	0.64 ± 0.03**	0.58 ± 0.02**	immune response
Q24JW2	lysozyme	0.39 ± 0.08*	0.39 ± 0.24	immune response
Q6PFU1	CD81 antigen	0.62 ± 0.04*	0.62 ± 0.13	immune response
Q7ZVM6	cytotoxic granule-associated RNA binding protein 1, like	1.18 ± 0.18	1.43 ± 0.03*	immune response
Q6PHG2	hemopexin	0.58 ± 0.11	0.50 ± 0.05*	inflammatory response
Response to Stress				
F1QUW4	hypoxia up-regulated protein 1	1.29 ± 0.25	1.27 ± 0.03*	response to hypoxia
Q90486	hemoglobin subunit beta-1	0.62 ± 0.04*	0.84 ± 0.24	response to hypoxia
E9QH31	aldehyde dehydrogenase	1.21 ± 0.03*	1.22 ± 0.05	oxidoreductase activity
F1QUR3	protein disulfide-isomerase (Fragment)	1.30 ± 0.21	1.44 ± 0.10*	protein folding

DOI: 10.1021/acs.est.6b03990
Environ. Sci. Technol. 2017, 51, 596−607

Table 1. continued

protein accession[a]	protein description	fold change[b] 1 μg/L	fold change[b] 10 μg/L	function category
Response to Stress				
Q6NYZ0	Dnajb11 protein	1.27 ± 0.23	1.28 ± 0.03**	protein folding
Q6PE26	Calr protein	1.56 ± 0.34	1.47 ± 0.05**	protein folding
Q7ZZA3	peptidyl-prolyl cis−trans isomerase	1.50 ± 0.11*	1.20 ± 0.10	protein folding
Z4YIA7	calumenin-A	1.51 ± 0.22	1.48 ± 0.04*	protein folding
Other Function				
Q7SXF6	cysteine-rich with EGF-like domain protein 2	1.40 ± 0.40	1.39 ± 0.03**	calcium ion binding
Q7ZT36	parvalbumin 3	0.74 ± 0.03*	1.12 ± 0.27	calcium ion binding
E9QB46	selenium-binding protein 1	1.34 ± 0.09	1.44 ± 0.04*	selenium binding
Q6DGU5	solute carrier family 25 member 46	0.81 ± 0.01*	0.84 ± 0.01	mitochondrial membrane fission; transport
F1QT89	reticulon	1.13 ± 0.11	1.24 ± 0.03*	membrane morphogenesis
Q5U3G0	progesterone receptor membrane component 1	1.35 ± 0.12	1.62 ± 0.07**	progesterone receptor
Q64HD0	sex hormone binding globulin	0.71 ± 0.02*	0.79 ± 0.08	sex hormone transport
F1QRA6	tetratricopeptide repeat protein 38	0.93 ± 0.11	0.73 ± 0.02*	unknown
Q8AW82	novel protein similar to human proliferation-associated 2G4 protein (PA2G4)	1.22 ± 0.02*	1.03 ± 0.03	growth regulation

[a]More information on proteins that were up- or down-regulated are listed in SI Table S2. [b]The fold changes are indicated as compared to the controls. Values >1 indicate up-regulation, and values <1 indicate down-regulation. Proteins with fold difference >1.2 or <0.83 and $p < 0.05$ were considered significantly altered, which are indicated with * ($p < 0.05$) or ** ($p < 0.01$).

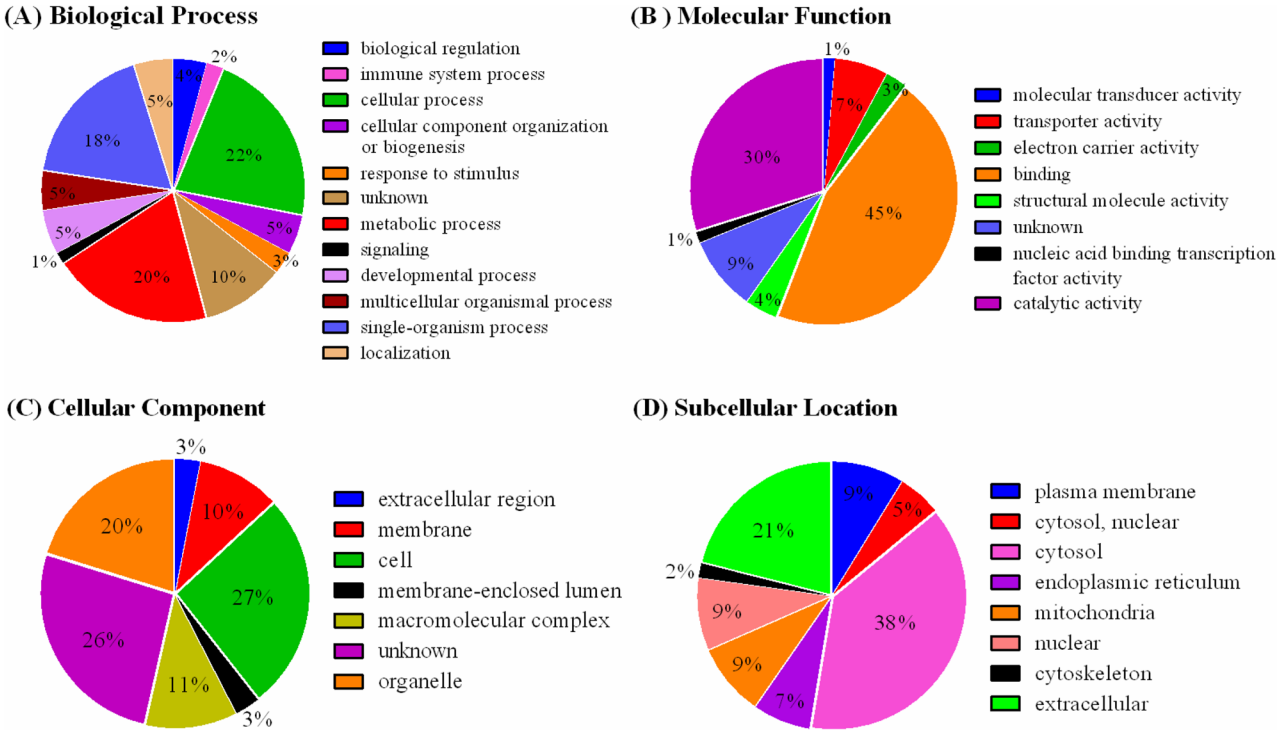

Figure 2. Classification of differentially expressed proteins (with functional annotation) in liver of zebrafish exposed to MC-LR based on (A) biological processes, (B) molecular function, (C) cellular component, and (D) subcellular location.

stable and unaffected by exposure to MC-LR. Therefore, they were used as the endogenous assay control. Geometric means of expression level of *gapdh* and *18S rRNA* were used to normalize qRT-PCR data.[39]

Statistical Analyses. Statistical analyses of the data were performed using SPSS package16.0 (SPSS, Chicago, IL). All values were presented as the mean ± standard error (SE). The Kolmogorov−Smirnov test and Levene's test were employed to check normality and homogeneity of variances in the data, respectively. If necessary, data were log-transformed to approximate normality. Nonparametric analysis was conducted if data could not meet the normality even after transformation. One-way analysis of variance (ANOVA) and Tukey's multiple comparison tests were applied to determine statistical differences between data of the control and MC-LR treatment groups. Significant differences were set at the $p < 0.05$ (*) and $p < 0.01$(**) levels.

DOI: 10.1021/acs.est.6b03990
Environ. Sci. Technol. 2017, 51, 596−607

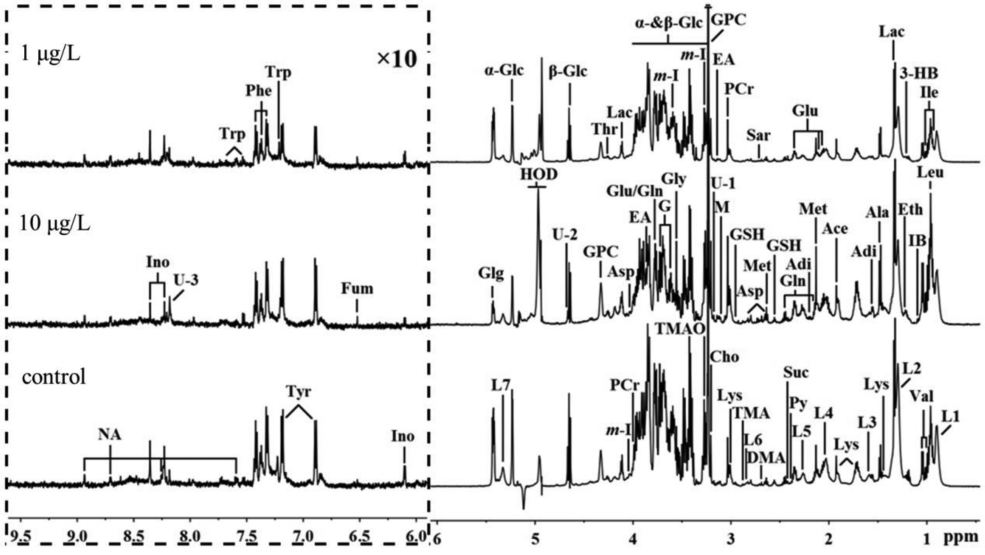

Figure 3. Typical ^{1}H HR-MAS CPMG NMR spectra (δ0.5−6.0 and δ6.0−9.5) of liver of zebrafish exposed to MC-LR. The region of δ6.0−9.5 (in the dashed box) in the aquatic phase was magnified 10 times compared with corresponding region of δ0.5−6.0 for the purpose of clarity. Keys: 3-HB: 3-hydroxybutyrate; Ace: acetate; Adi: adipate; Ala: alanine; Asp: aspartate; Cho: choline; DMA: dimethylamine; EA: ethanolamine; Eth: ethanol; Fum: fumarate; G: glycerol; Glc: glucose; Glg: glycogen; Gln: glutamine; Glu: glutamate; Gly: glycine; GPC: glycerolphosphocholine; GSH: glutathione; IB: isobutyrate; Ile: isoleucine; Ino: inosine; L1: LDL&VLDL, CH_3-$(CH_2)_n$-; L2: LDL&VLDL, CH_3-$(CH_2)_n$-; L3: VLDL, $-CH_2-CH_2-C{=}O$; L4: Lipid, $-CH_2-CH{=}CH$-; L5: Lipid, $-CH_2-C{=}O$; L6: Lipid, $=CH-CH_2-CH=$; L7: lipid, $-CH{=}CH$-; Lac: lactate; Leu: leucine; Lys: lysine; M: malonate; Met: methionine; *m*-I: *myo*-inositol; Mol: methanol; NA: nicotinamide; PCr: phosphocreatine; Phe: phenylalanine; Py: pyruvate; Sar: sarcosine; Suc: succinate; Thr: threonine; TMA: trimethylamine; TMAO: trimethylamine N-oxide; Trp: tryptophan; Tyr: tyrosine; U: unknown; Val: valine.

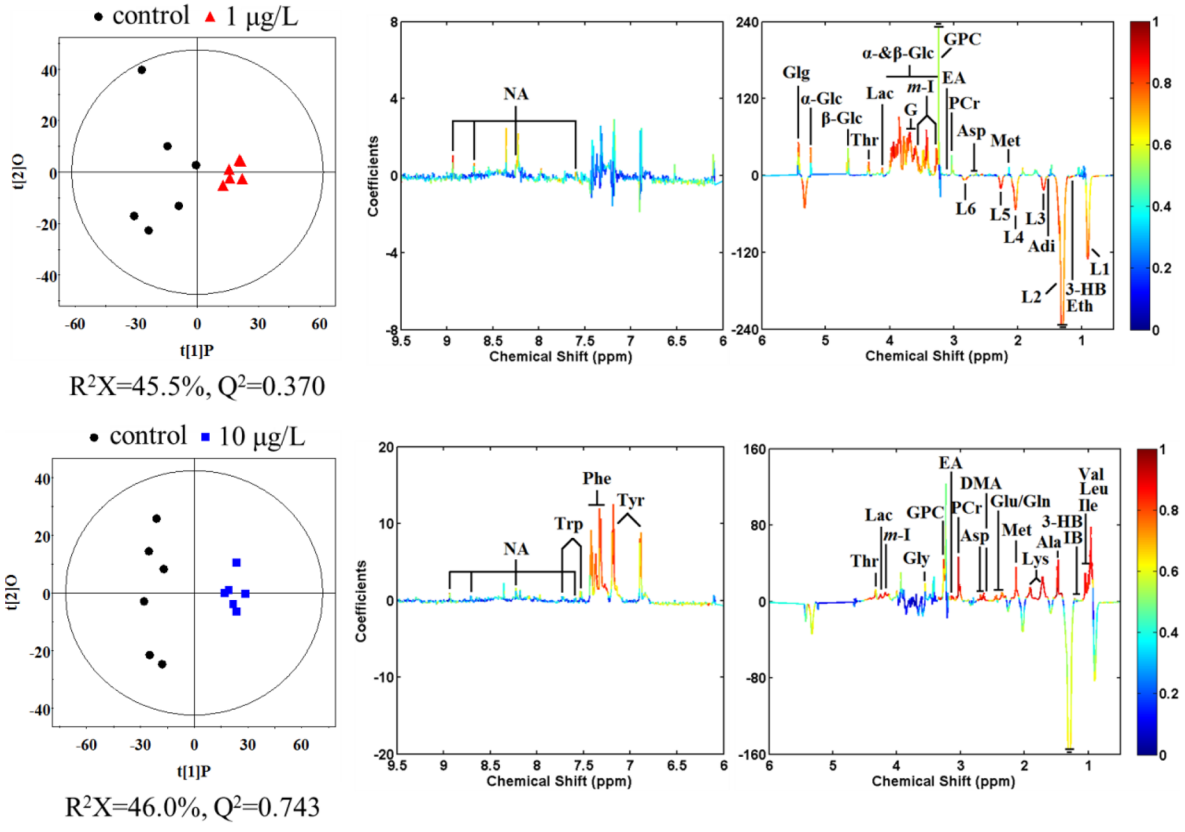

Figure 4. OPLS-DA score plots (left panel) derived from ^{1}H CPMG NMR spectra of liver of zebrafish exposed to MC-LR and corresponding coefficient loading plots (right panel) obtained from different groups. The color map shows the significance of variation among metabolites between the two classes. Peaks in the positive direction (up) indicate metabolites that are more abundant in the MC-LR treatment groups than in the control group. Consequently, metabolites that are more abundant in the control group are presented as peaks in the negative direction (down). Keys of the assignments were shown in Figure 3.

DOI: 10.1021/acs.est.6b03990
Environ. Sci. Technol. 2017, 51, 596−607

Table 2. OPLS-DA Coefficients Derived from NMR Data for Metabolites in Liver of Zebrafish Exposed to MC-LR

metabolites	r^a 1 μg/L	r^a 10 μg/L	metabolites	r^a 1 μg/L	r^a 10 μg/L
3-HB: 3-hydroxybutyrate: 1.21(d[b])	−0.86	0.90	L6: lipid, =CH−CH_2−CH=: 2.82(br)	−0.79	–
Ace: acetate: 1.92(s)	–	0.85	Lac: lactate: 1.33(d), 4.11(q)	0.80	0.82
Adi: adipate: 1.56(m), 2.18(m)	−0.77	0.91	Leu: leucine: 0.96(t)	–	0.86
Ala: alanine: 1.48(d)	–	0.89	Lys: lysine: 1.72(m), 1.91(m), 3.02(m), 3.76(t)	–	0.91
Asp: aspartate: 2.67(dd), 2.81(dd), 3.95(dd)	0.81	0.91	M: malonate: 3.11(s)	–	0.89
DMA: dimethylamine: 2.72(s)	–	0.92	Met: methionine: 2.14(s), 2.64(t)	0.77	0.91
EA: ethanolamine: 3.13(t), 3.87(t)	0.78	0.87	m-I: myo-inositol: 3.26(t), 3.62(m), 4.07(m)	0.86	0.81
Eth: ethanol: 1.19(t)	−0.86	–	Mol: methanol: 3.36(s)	0.80	–
G: glycerol: 3.58(m), 3.68(m)	0.86	–	NA: nicotinamide: 7.59(m), 8.25(m), 8.71(d), 8.93(s)	0.93	0.77
Glg: glycogen: 3.97(m), 5.42(m)	0.81	–	PCr: phosphocreatine: 3.04(s), 3.93(s)	0.89	0.93
Gln: glutamine: 2.12(m), 2.45(m), 3.78 (t)	–	0.86	Phe: phenylalanine: 7.32(d), 7.37(t), 7.42(m)	–	0.82
Glu: glutamate: 2.07(m), 2.12(m), 2.35(m), 3.78(t)	–	0.86	Py: pyruvate: 2.38(s)	–	0.86
Gly: glycine: 3.56(s)	0.87	0.78	Sar: sarcosine: 2.73(s)	–	0.89
GPC: glycerolphosphocholine: 3.23(s), 4.33(m)	0.79	0.78	Suc: succinate: 2.42(s)	–	0.79
GSH: glutathione: 2.56(m), 2.95(m)	0.82	0.82	Thr: threonine: 4.26(m)	–	0.89
IB: isobutyrate: 1.09(d)	–	0.83	TMAO: trimethylamine N-oxide: 3.27(s)	0.86	–
Ile: isoleucine: 0.94(t), 1.01(d)	–	0.90	Trp: tryptophan: 7.53(d), 7.73(d)	–	0.81
L1: LDL&VLDL, CH_3-$(CH_2)_n$-: 0.90(br)	−0.78	–	Tyr: tyrosine: 6.89(d), 7.19(d)	–	0.81
L2: LDL&VLDL, CH_3-$(CH_2)_n$-: 1.30(br)	−0.83	–	Val: valine: 0.99(d), 1.04(d)	–	0.89
L3: VLDL, −CH_2−CH_2−C=O: 1.59(br)	−0.80	–	α-Glc: α-glucose: 3.42(t), 3.54(dd), 3.72(t), 3.74(m), 3.84(m), 5.23(d)	0.86	–
L4: Lipid, −CH_2−CH=CH-: 2.02(br)	−0.76	–	β-Glc: β-glucose: 3.25(dd), 3.41(t), 3.46(m), 3.49(t), 3.90(dd), 4.65(d)	0.88	–
L5: Lipid, −CH_2−C=O: 2.26(br)	−0.87	–			

[a]Correlation coefficients, positive and negative signs indicate positive and negative correlation in the concentrations, respectively. The correlation coefficient of |r|> 0.755 was used as the cutoff value for the statistical significance based on the discrimination significance at the level of $p = 0.05$ and df (degree of freedom) = 5. "–" means the correlation coefficient |r| is less than 0.755. [b]Multiplicity: s, singlet; d, doublet; t, triplet; q, quartet; dd, doublet of doublets; m, multiplet; br, broad resonance.

RESULTS

Actual Concentrations of MC-LR in Water. Measured concentrations of MC-LR in water were 0.82 ± 0.08 (from 0.69 to 1.02), 8.45 ± 0.71 (from 7.34 to 9.83) μg/L, respectively, for the nominal 1 and 10 μg/L MC-LR groups (SI Figure S2). No MC-LR was detected in control water.

Light Microscopy and Ultrastructural Observations. No histological changes were observed in livers of fish from the control group (Figure 1A and D). However, in livers of fish exposed to 1 μg MC-LR/L (Figure 1B and E), cord-like parenchymal architecture of liver was lost and some cytoplasmic inclusions were no longer observable. Swelling of hepatic cells and hepatocellular vacuolar degeneration were observed. Hepatic lesions were more severe in fish exposed to 10 μg MC-LR/L (Figure 1C and F) and cells were nearly collapsed. Similarly, observations of ultrastructure also showed that MC-LR caused histological damage to the liver. Liver cells showed cytoplasmic shrinkage, dilation of rough endoplasmic reticulum and swollen mitochondria occurred in livers of fish exposed to 1 μg MC-LR/L (Figure 1H and I). In livers of fish exposed to 10 μg MC-LR/L (Figure 1J, K and L), some vacuoles, swollen mitochondria and hyperplasia of smooth endoplasmic reticulum associated with mild expansion were also observed. Numerous lysosomes were present in the cytoplasm, and autophagic vacuoles were also detected.

Proteome Analysis. In total, 2,761 proteins were identified of which 1,966 proteins could be quantified by use of iTRAQ labeling and HPLC fractionation followed by LC-MS/MS analysis. Among those quantified, 37 and 81 proteins were up- and down-regulated by exposure to 1 or 10 μg MC-LR/L, respectively (SI Table S2). All annotated proteins that were up- or down-regulated are listed (Table 1), including proteins involved in mitochrondrial energy metabolism (NADH dehydrogenase (Ubiquinone) flavoprotein 1, cytochrome c oxidase submit 2), lipid metabolism (acetoacetyl-CoA synthetase, apolipoprotein Eb), and endoplasmic reticulum stress (Calumenin-A, Dnajb11 protein), etc. Full details of the altered proteins are given (SI Table S3). Differentially expressed proteins were classified into various categories (Figure 2). When these regulated proteins were classified according to biological process, regulated proteins were mostly involved in cellular (22%), metabolic (20%), or single-organism process (18%) (Figure 2A). Affected proteins covered a wide range of molecular functions, mainly including catalytic activity (30%) and binding (45%) (Figure 2B). Based on classification by cellular components, many proteins were in organelles (20%) or cells (27%) (Figure 2C). Most proteins were located in the cytosol (38%), extracellular region (21%), nucleus (9%), mitochondria (9%), and plasma membrane (9%) (Figure 2D).

Metabolome Analysis. Typical ^{1}H NMR spectra of livers of zebrafish exposed to 0, 1, or 10 μg MC-LR/L are presented (Figure 3). PCA was performed to provide an overview of ^{1}H CPMG NMR data from all samples. PCA score plots (SI Figure S3) demonstrated some separation between control and MC-treated groups. Separation between controls and those exposed to 10 μg MC-LR/L was especially obvious. PLS-DA was further applied to achieve separation profiles of the various treatments through maximizing intergroup variance. Results from both permutation tests and cross validation parameter Q^2 suggested that models constructed from spectral data of zebrafish liver were valid and strong (Figure S4). In order to understand

DOI: 10.1021/acs.est.6b03990
Environ. Sci. Technol. 2017, 51, 596−607

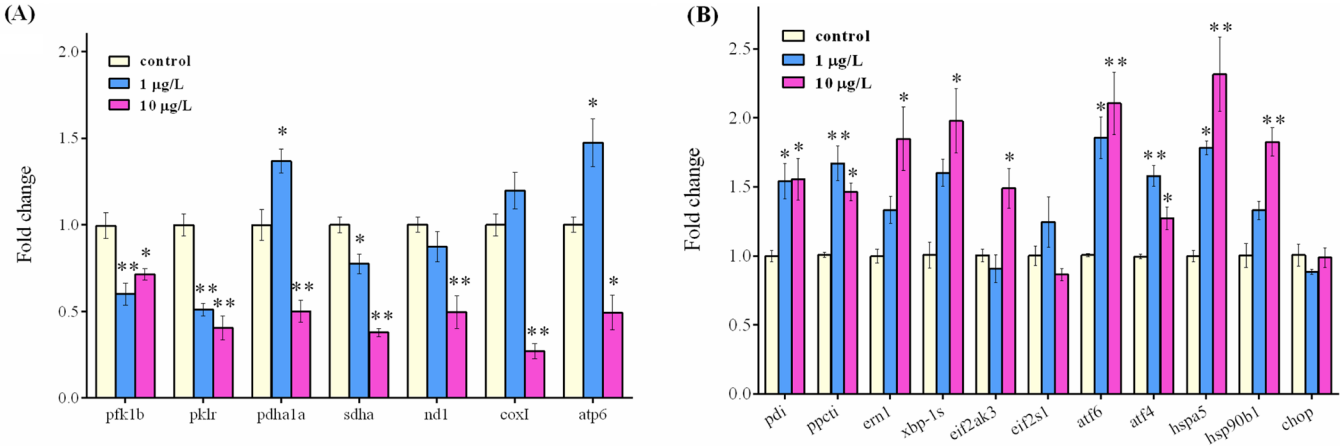

Figure 5. Expression of genes involved in energy metabolism and endoplasmic reticulum stress (ERS) in livers of zebrafish exposed to 1 or 10 μg MC-LR/L for 90 days. (A) genes involved in glycolysis (*pfk1b, pklr*), tricarboxylic acid cycle (*pdha1a, sdha*), electron transport chain (*nd1, coxI*), and oxidative phosphorylation (*atp6*), (B) genes involved in protein folding (*pdi, ppcti*) and ERS (*ern1, xbp-1s, eif2ak3, eif2s1, atf6, atf4, hspa5, hsp90b1, chop*).Quantitative real-time PCR was used to test the expression levels of target genes. *Gapdh* and *18S rRNA* were used as internal controls. Values are presented as the mean ± standard error (SE). * indicates $p < 0.05$ versus control, and ** indicates $p < 0.01$ versus control.

differences in profiles of metabolites in fish exposed to MC-LR, metabolic profiles obtained from individuals exposed to MC-LR or controls were further analyzed by use of OPLS-DA. The OPLS-DA score plots and corresponding loading plots based on the NMR data of liver tissue for the pairwise groups are presented in Figure 4. The OPLS-DA score plots (left panel in Figure 4) give a clear separation between MC-treated groups and the corresponding controls, and the color-coded coefficient plots (right panel in Figure 4) revealed detailed metabolic changes induced by MC-LR. The dominant metabolites contributing to separation between the control and groups exposed to MC-LR are listed (Table 2). The elevation of intermediate metabolites in energy metabolism (pyruvate, lactate, succinate) and amino acids (alanine, glycine, methionine, etc.), reduction of lipid metabolites (glycerol, lipid, $-CH_2-C{=}O$, $-CH_2-CH{=}CH-$, etc.) were observed in liver of zebrafish exposed to 1 or 10 μg MC-LR/L.

Expressions of Genes. Changes in transcription of genes involved in glycolysis (*pfk1b, pklr*), tricarboxylic acid cycle (*pdha1a, sdha*), electron transport chain (*nd1, coxI*), and oxidative phosphorylation (*atp6*) are shown (Figure 5A). All of these genes were significantly down-regulated in livers of zebrafish exposed to 10 μg MC-LR/L. For fish exposed to 1 μg MC-LR/L, levels of mRNA for of *pdha1* and *atp6* were greater while there were no differences in levels of mRNA for *nd1* or *coxI*. At this concentration of MC-LR, levels of mRNA for *pfk1b, pklr* and *sdha* were significantly less.

Alterations of transcripts of genes that encode proteins important for protein folding (*pdi, ppcti*) and endoplasmatic reticulum stress (*ern1, xbp-1s, eif2ak3, eif2s1, atf6, atf4, hspa5, hsp90b1, chop*) are shown (Figure 5B). Abundances of transcripts of *pdi, ppcti, atf6, atf4, hspa5* were significantly greater in fish exposed to 1 μg MC-LR/L, relative to the unexposed controls. In individuals esposed to 10 μg MC-LR/L, there were greater levels of mRNA for *pdi, ppcti, ern1, xbp-1s, eif2ak3, atf6, atf4, hspa5, hsp90b1*, but no obvious changes for mRNA of eif2s1 or *chop*.

DISCUSSION

Concentrations of MC-LR used in the study, results of which are presented here, were chosen to represent those likely to occur in aquatic environments and were less than those expected to cause overt toxicity or lethality. No lethality was observed during exposures to MC-LR, which indicated that exposures were indeed less than the threshold for overt toxic effects on general health of exposed fish. However, damage to liver was observed by use of histology. This finding potentially has implications for long-term health of fish (and other aquatic animals) which are exposed throughout their lives to environmentally relevant concentrations of MCs.

Under normal conditions, the major source of energy supply is oxidative metabolism of nutrients through aerobic respiration; while under hypoxia, the major energy supply is shifted to anoxic respiration, which is less efficient at producing energy than is aerobic respiration. Gill tissue, which comes into direct and immediate contact with MCs in water, is vulnerable to effects of MC-LR.[28,40] Because gills are respiratory organs of fish, damage to that organ would cause limitations of efficiency on exchanges of gases and ions, and result in insufficient oxygen transfer from water into the body and ultimately the bloodstream, thus producing hypoxia. Coincidentally, the proteomic analysis also showed that hemoglobin subunit beta-1 was less while hypoxia up-regulated protein 1 was greater in fish exposed to MC-LR, which suggested that exposure to MC-LR might induce hypoxia.[41,42] Results of the metabolomic analysis supported these findings, with lactate being up-regulated in response to exposure to MC-LR. Lactate results from glycolysis and its increase is indicative of a shift of energy metabolism from aerobic respiration to anaerobic respiration. Changes in amounts of several metabolites, related to energy transformations, such as accumulation of pyruvate, which is an end product of glycolysis, and succinate, which is an intermediate of the tricarboxylic acid (TCA) cycle, were also observed in livers of fish exposed to 10 μg MC-LR/L. Expressions of NADH dehydrogenase (Ubiquinone) flavoprotein 1 (NDUFV1) and cytochrome c were down-regulated (0.69-, 0.70-fold, respectively) in livers of fish exposed to 10 μg MC-LR/L, whereas cytochrome c oxidase submit 2 (COX2) was up-regulated (1.21-fold) in livers of individuals exposed to 1 μg MC-LR/L. NDUFV1, the core subunit of the mitochondrial membrane respiratory chain NADH dehydrogenase (Complex I), is a potent source of reactive oxygen

DOI: 10.1021/acs.est.6b03990
Environ. Sci. Technol. 2017, 51, 596−607

species (ROS), and its decrease might contribute to a deficit in bioenergy or cause damage from oxidative stress.[43,44] Cytochrome c (cyt c) is an essential component of the electron transport chain (ETC) in mitochondria and transfers electrons between Complexes III (Coenzyme Q - cyt c reductase) and IV (cyt c oxidase), the terminal enzyme of mitochondrial ETC.[45] To further evaluate effects of MC-LR on energy metabolism, real-time PCR was used to analyze transcription of several genes involved in glycolysis (*pfk1b*, *pklr*), TCA cycle (*pdha1*, *sdha*), ETC (nd1, sdha, coxI), and oxidative phosphorylation (*OXPHOS*, *atp6*). Expressions of mRNA for these genes were less in fish exposed to MC-LR relative to those in controls not exposed to MC-LR, which indicated that the energy generating system of zebrafish was significantly impaired. Results of previous studies have shown that MC-LR caused disorder in mitochondrial ETC and OXPHOS systems of testis of rat and liver of crucian carp.[34,46] In the present study, swollen mitochondria were also observed in livers of zebrafish exposed to MC-LR. Impairment of mitochondria and depletion of energy reserves would affect abilities of organisms to repair damage to cells or proteins, due to exposure to MCs. Free amino acids can be involved in both osmotic regulation and energy metabolism. In this study, several amino acids were greater in livers of zebrafish exposed to 10 μg MC-LR/L, which confirmed altered energy metabolism.

In fish, lipids and fatty acids are preferred sources of energy, in contrast to mammals which use carbohydrates.[47] In this study, significantly greater concentrations of glycerol and lesser concentrations of L1: LDL&VLDL, CH_3-$(CH_2)_n$-, L2: LDL&VLDL, CH_3-$(CH_2)_n$-, L3:VLDL, $-CH_2-CH_2-C{=}O$, L4: Lipid, $-CH_2-CH{=}CH$-, L5: Lipid, $-CH_2-C{=}O$, and L6: Lipid, $=CH-CH_2-CH=$ observed in livers of fish exposed to 1 μg MC-LR/L represented the disordering of metabolism of lipids in liver. Moreover, the proteomic analysis also showed that several proteins involved in metabolism of lipids, such as Acetoacetyl-CoA synthetase, Apolipoprotein Eb, Fatty acid-binding protein 10-A, liver basic, and Acbd7 protein were up-regulated or down-regulated. These results are consistent with the reported toxicological effects of MCs on metabolism of lipids.[28,48,49]

CDIPT (CDP-diacylglycerol-inositol 3-phosphatidyltransferase), also known as phosphatidylinositol synthase (PIS), is indispensable in synthesis of phosphatidylinositol (PtdIns) from CDP-DAG and myo-inositol in endoplasmic reticula.[50] Phosphorylated derivatives of PtdIns, phosphoinositides (PIs), are crucial regulators of calcium homeostasis, membrane trafficking, secretory pathways, signal transduction, and lipid metabolism. In this study, CDIPT was up-regulated while phosphoinositide phospholipase C (PLC) was down-regulated. Previous studies demonstrated that cdipt-deficient zebrafish exhibit endoplasmic reticulum stress (ERS) in liver and steatosis.[50] A recent study showed that MC-LR altered mRNA and protein expression of ERS signaling molecules (PERK and ATF6) related to hepatic lipid metabolism abnormalities in mice.[51]

The endoplasmic reticulum (ER) is one of the largest cellular organelles and is responsible for regulation of synthesis, folding and targeting of proteins as well as metabolism of lipids and overall maintenance of calcium homeostasis. In the case of an ER disturbance, whether through alteration of concentrations of calcium, oxidative stress or disruption of energy balance, all of which were observed previously due to exposure to MCs, influx of unfolded or misfolded peptides exceeded capacity of ER to fold and/or process, ER stress (ERS) would be triggered.[52−54] To combat ERS, cells have evolved a highly conserved adaptive response, referred to as the unfolded protein response (UPR), by increasing production of protein chaperones needed for proper folding of proteins or if unsuccessful by degrading unfolded proteins. Formation of correct disulfide bonds between cysteine (Cys) residues and the cis−trans isomerization of peptide bonds preceding proline (Xaa-Pro bonds) are the rate-determining processes in folding of some proteins, which can be accelerated by protein disulfide isomerase (PDI) and peptidyl-prolyl cis−trans isomerase (PPI), respectively.[55] However, both of these enzymes were shown to be up-regulated, suggesting that protein folding was disturbed by prolonged exposure to MC-LR. Apart from PDI and PPI, several proteins involved in ERS and UPR, including Calumenin-A, Dnajb11 protein, Calr protein, Cysteine-rich with EGF-like domain protein 2, were up-regulated. Results of real-time PCR also showed that transcription of genes involved in protein folding (*pdi*, *ppcti*) and endoplasmatic reticulum stress (*ern1*, *xbp-1s*, *eif2ak3*, *atf6*, *atf4*, *hspa5*, *hsp90b1*) were greater in individuals exposed to MC-LR, relative to those in unexposed control individuals. The results of the study presented here revealed that ERS plays a role in disruption of metabolism of lipids in livers of zebrafish exposed to MC-LR. Results of previous studies have shown that exposure to MC-LR induced ERS and UPR in liver of zebrafish and mice, and human hepatoma HepG2 and Huh7 cells.[51,54,56−59] However, since a longer exposure was performed in this study, the zebrafish might be unable to alleviate ERS such that ER-associated degradation occurred. Greater concentrations of free amino acids observed by metabolomics might have also resulted from MC-induced protein degradation and/or the process of cellular injury and repair itself.

The organic osmolytes, myo-inositol, trimethylamine N-oxide (TMAO), and glycerophosphocholine (GPC) were significantly greater in livers of zebrafish exposed to MC-LR. Severe histopathological change (cell shrinkage) in livers of fish exposed to MC-LR, was indicative of disrupted osmotic balance. During cell shrinkage, cells accumulate osmolytes to adapt to changes in cell volume, but this process is metabolically expensive.[60] Thus, increases of myo-inositol, TMAO and glycerophosphocholine might be an attempt of fish to maintain intracellular homeostasis.

S-adenosylmethionine synthase (methionine adenosyltransferase, MAT), the unique enzyme responsible for synthesis of S-adenosylmethionine (SAMe) from methionine and adenosine triphosphate (ATP), was significantly down-regulated in livers of fish exposed to MC-LR, whereas the concentration of methionine was greater. SAMe is the principal biological donor of methane and plays a critical role in maintaining normal hepatic function.[61] It can also regulate glutathione (GSH) levels through the trans-sulfuration pathway. Results of our previous studies also demonstrated that concentrations of both MAT1a and GSH were significantly less in livers of rats exposed to MC-LR, which resulted in a decoupling of the detoxification system and making cells more susceptible to oxidative stress.[62,63] However, concentrations of GSH were greater in livers of zebrafish exposed to MC-LR, which can explain the greater tolerances of fish to MCs than mammalians.[64] MCs have been previously shown to bind to cysteine (Cys) residues of proteins in liver and it is likely that induction of protein disulfide

DOI: 10.1021/acs.est.6b03990
Environ. Sci. Technol. 2017, 51, 596−607

isomerase (PDI) is involved in cellular detoxification to formation of MC-Cys conjugation with proteins.[65]

Given the fact that osmotic regulation, unfolded protein response, GSH synthesis, and excretion of MCs are energy-dependent, accumulation of osmolytes and detoxification might aggravate energy deficiency induced by MCs. However, phosphocreatine (PCr) was significantly greater in livers of zebrafish exposed to either 1 or 10 μg MC-LR/L, compared with that of controls. PCr is used as an emergency energy source, donating one phosphate group to adenosine diphosphate (ADP) to supply unmet ATP need.[60] Glycogen and α- and β-glycose, were also greater in livers of zebrafish exposed to 1 μg MC-LR/L. Thus, greater concentrations of PCr, glycogen and glycose represented a protective mechanism to counteract deficiency in energy caused by exposure to MC-LR and qualified as biomarkers for toxicity of MC-LR.

One unexpected observation in proteomic analysis was that exposure to MC-LR can down-regulate expression of serine/threonine-protein phosphatase 2A catalytic subunit (PP2A C subunit). Covalent binding and inhibition of PP1 and PP2A is widely assumed to be the principal mechanism by which MCs cause toxicity, which in turn causes excessive phosphorylation of proteins.[66,67] Results of several studies, which were inconsistent with our study, have shown that MC-LR up-regulated expression of PP2A C subunit in Huh7 cells and zebrafish larvae and increased PP activities in liver and brain of zebrafish after acute or subchronic exposure[27,44,59,68] This could potentially have resulted from differences in species-, organ-, cell- sensitivities and/or difference between chronic exposure and acute/subchronic exposure. It is also possible that chronic exposure to MC-LR can modulate expression of protein phosphatase rather than serving the previously predicted structural roles as a molecular scaffold. Therefore, the finding that MC-LR can down-regulate expression of the PP2A C subunit observed in the present study might deepen our understanding of its toxicity mechanisms.

Four proteins including histone 2A (H2A), histone 3 (H3), histone deacetylase 8, acidic leucine-rich nuclear phosphoprotein 32 family member E (ANP32E) were significantly different in livers of zebrafish exposed to 1 or 10 μg MC-LR/L. Histones are primary protein components of chromatin, acting as spools around which DNA winds, thus enabling compaction necessary to fit large genomes of eukaryotes inside their nuclei. ANP32E is an H2A.Z chaperone, specifically able to remove H2A.Z from the nucleosome.[69] Modifications of histones, including acetylation and deacetylation act in diverse biological processes, such as regulation of transcription, repair of DNA, and condensation of chromosomes.[70,71]

In summary, this is the first study revealing that chronic exposure to MC-LR cause damage of liver of a model fish species, zebrafish. Using combined proteomics and metabolomics, we have provided detailed molecular information, at both regulatory and functional levels, on the responses of zebrafish to MC exposure. MC-LR significantly caused dysfunctions of mitochondria and caused a switch from aerobic to anaerobic respiration. In addition, endoplasmic reticulum stress contributed to disturbance of metabolism of lipids in liver of zebrafish exposed to MC-LR.

■ ASSOCIATED CONTENT

Supporting Information

The Supporting Information is available free of charge on the ACS Publications website at DOI: 10.1021/acs.est.6b03990.

(1) iTRAQ-based quantitative proteomic analysis; (2) HR-MAS ^{1}H NMR-based metabolomic analysis; (3) Table S1. qRT-PCR primer sequences for selected genes; (4) Table S2. Number of altered proteins; (5) Table S3. Differentially expressed proteins (with functional annotation); (6) Figure S1. Quality control validation of mass spectrometry data; (7) Figure S2. Concentrations of MC-LR; (8) Figure S3. PCA score plots; (9) Figure S4. PLS-DA score plots and cross validation by permutation test (PDF)

■ AUTHOR INFORMATION

Corresponding Authors

*(J.C.) Phone/fax: +86-27-68780622; e-mail: chenjun@ihb.ac.cn.

*(P.X.) E-mail: xieping@ihb.ac.cn.

ORCID

Liang Chen: 0000-0001-6548-5000

Author Contributions

#These authors contributed equally to this work.

Notes

The authors declare no competing financial interest.

■ ACKNOWLEDGMENTS

We thank Dr. Gerald Ankley and three anonymous reviewers for their very helpful and constructive comments that greatly improved the manuscript. Thanks to Dr. Li Li from College of Fisheries, Huazhong Agricultural University for her help in histology analysis. We are grateful to Drs. Jiayin Dai and Hongxia Zhang from Institute of Zoology, Chinese Academy of Sciences and Dr. Qian Xiong from Institute of Hydrobiology, Chinese Academy of Sciences for their help in data analysis of proteomics. We also thank Dr. Hongbing Liu from Wuhan Institute of Physics and Mathematics, Chinese Academy of Sciences for his kind help in NMR experiment and data analysis. This work was supported by the Excellent Young Scientists Fund, National Natural Science Foundation of China (grant number 31322013), and State Key Laboratory of Freshwater Ecology and Biotechnology (grant number 2016FBZ08). Prof. John P. Giesy was supported by "High Level Foreign Experts" program (#GDT20143200016) funded by the State Administration of Foreign Experts Affairs, China to Nanjing University and Einstein Professor Program of Chinese Academy of Sciences. Giesy was also supported by Canada Research Chair program and a Distinguished Visiting Professorship in School of Biological Sciences, University of Hong Kong.

■ REFERENCES

(1) Merel, S.; Walker, D.; Chicana, R.; Snyder, S.; Baurès, E.; Thomas, O. State of knowledge and concerns on cyanobacterial blooms and cyanotoxins. *Environ. Int.* **2013**, *59*, 303−327.

(2) Wood, R. Acute animal and human poisonings from cyanotoxin exposure - A review of the literature. *Environ. Int.* **2016**, *91*, 276−282.

(3) Chen, J.; Xie, P.; Li, L.; Xu, J. First identification of the hepatotoxic microcystins in the serum of a chronically exposed human population together with indication of hepatocellular damage. *Toxicol. Sci.* **2009**, *108*, 81−89.

(4) Li, Y.; Chen, J.-A.; Zhao, Q.; Pu, C. W.; Qiu, Z. Q.; Zhang, R. P.; Shu, W. Q. A cross-sectional investigation of chronic exposure to microcystin in relationship to childhood liver damage in the Three Gorges Reservoir Region, China. *Environ. Health Perspect.* **2011**, *119*, 1483−1488.

(5) Lin, H.; Liu, W. Y.; Zeng, H.; Pu, C. W.; Zhang, R. P.; Qiu, Z. Q.; Chen, J.-A.; Wang, L. Q.; Tan, Y.; Zheng, C. F.; Yang, X. H.; Tian, Y. Q.; Huang, Y. J.; Luo, J. H.; Luo, Y.; Feng, X. B.; Xiao, G. S.; Feng, L.; Li, H.; Wang, F.; Yuan, C. Y.; Wang, J.; Zhou, Z. Y.; Wei, T. T.; Zuo, Y. L.; Wu, L. P.; He, L. X.; Guo, Y. P.; Shu, W. Q. Determination of environmental exposure to microcystin and aflatoxin as a risk for renal function based on 5493 rural people in Southwest China. *Environ. Sci. Technol.* **2016**, *50*, 5346−5356.
(6) Zhao, Y. Y.; Xue, Q. J.; Su, X. M.; Xie, L. Q.; Yan, Y. J.; Wang, L. X.; Steinman, A. D. First identification of the toxicity of microcystins on pancreatic islet function in humans and the involved potential biomarkers. *Environ. Sci. Technol.* **2016**, *50*, 3137−3144.
(7) Niedermeyer, T. Microcystin congeners described in the literature. 2013. Available online: http://dx.doi.org/10.6084/m9.figshare.880756 (accessed on 21 October 2014).
(8) Puddick, J.; Prinsep, M. R.; Wood, S. A.; Kaufononga, S. A. F.; Cary, S. C.; Hamilton, D. P. High levels of structural diversity observed in microcystins from *microcystis* CAWBG11 and characterization of six new microcystin congeners. *Mar. Drugs* **2014**, *12*, 5372−5395.
(9) Žegura, B.; Štraser, A.; Filipič, M. Genotoxicity and potential carcinogenicity of cyanobacterial toxins - a review. *Mutat. Res., Rev. Mutat. Res.* **2011**, *727*, 16−41.
(10) Singh, S.; Asthana, R. K. Assessment of microcystin concentration in carp and catfish: a case study from Lakshmikund pond, Varanasi, India. *Bull. Environ. Contam. Toxicol.* **2014**, *92*, 687−692.
(11) Nikitin, O. V.; Stepanova, N. Y.; Latypova, V. Z. Human health risk assessment related to blue-green algae mass development in the Kuibyshev Reservoir. *Water Sci. Technol.: Water Supply* **2015**, *15*, 693−700.
(12) Mohamed, Z. A.; Deyab, M. A.; Abou-Dobara, M. I.; El-Raghi, W. M. Occurrence of toxic cyanobacteria and microcystin toxin in domestic water storage reservoirs, Egypt. *Aqua* **2016**, *65*, 431−440.
(13) Chen, L.; Chen, J.; Zhang, X. Z.; Xie, P. A review of reproductive toxicity of microcystins. *J. Hazard. Mater.* **2016**, *301*, 381−399.
(14) Valério, E.; Vasconcelos, V.; Campos, A. New insights on the mode of action of microcystins in animal cells - A review. *Mini-Rev. Med. Chem.* **2016**, *16*, 1032−1041.
(15) WHO (World Health Organization). *Guidelines for Drinking-Water Quality*, 2nd ed, health criteria and other supporting information - addendum; World Health Organization: Geneva, 1998; Vol. *2*.
(16) *Toxic Cyanobacteria in Water: A Guide to Their Public Health Consequences, Monitoring and Management*; Chorus, I., Bartram, J. Eds.; E & FN Spon, London, on behalf of the World Health Organization: Geneva. 1999.
(17) IARC (International Agency for Research on Cancer). *IARC Monographs on the Evaluation of Carcinogenic Risks to Humans, Ingested Nitrate and Nitrite and Cyanobacterial Peptide Toxins*, Volume *94*, 2010.
(18) Pavagadhi, S.; Balasubramanian, R. Toxicological evaluation of microcystins in aquatic fish species: current knowledge and future directions. *Aquat. Toxicol.* **2013**, *142*−*143*, 1−16.
(19) Martins, J. C.; Vasconcelos, V. M. Microcystin dynamics in aquatic organisms. *J. Toxicol. Environ. Health, Part B* **2009**, *12*, 65−82.
(20) Amado, L. L.; Monserrat, J. M. Oxidative stress generation by microcystins inaquatic animals: Why and how. *Environ. Int.* **2010**, *36*, 226−235.
(21) Ferrão-Filho, A. S.; Kozlowsky-Suzuki, B. Cyanotoxins: bioaccumulation and effects on aquatic animals. *Mar. Drugs* **2011**, *9*, 2729−2772.
(22) Pavagadhi, S.; Gong, Z. Y.; Hande, M. P.; Dionysiou, D. D.; de la Cruz, A. A.; Balasubramanian, R. Biochemical response of diverse organs in adult *Danio rerio* (zebrafish) exposed to sub-lethal concentrations of microcystin-LR and microcystin-RR: A balneation study. *Aquat. Toxicol.* **2012**, *109*, 1−10.
(23) Malbrouck, C.; Kestemont, P. Effects of microcystins on fish. *Environ. Toxicol. Chem.* **2006**, *25*, 72−86.
(24) Mezhoud, K.; Praseuth, D.; Puiseux-Dao, S.; François, J.; Bernard, C.; Edery, M. Global quantitative analysis of protein expression and phosphorylation statusin the liver of the medaka fish (*Oryzias latipes*) exposed to microcystin-LR I.Balneation study. *Aquat. Toxicol.* **2008**, *86*, 166−175.
(25) Malécot, M.; Marie, A.; Puiseux-Dao, S.; Edery, M. iTRAQ-based proteomicstudy of the effects of microcystin-LR on medaka fish liver. *Proteomics* **2011**, *11*, 2071−2078.
(26) Phillips, M. J.; Roberts, R. J.; Stewart, J. A.; Codd, G. A. The toxicity of the cyanobacterium *Microcystis aeruginosa* to rainbow trout, *Salmo gairdneri* Richardson. *J. Fish Dis.* **1985**, *8*, 339−344.
(27) Wang, M. H.; Chan, L. L.; Si, M. Z.; Hong, H. S.; Wang, D. Z. Proteomic analysis of hepatic tissue of zebrafish (*Danio rerio*) experimentally exposed to chronic microcystin-LR. *Toxicol. Sci.* **2010**, *113*, 60−69.
(28) Pavagadhi, S.; Natera, S.; Roessner, U.; Balasubramanian, R. Insights into lipidomic perturbations in zebrafish tissues upon exposure to microcystin-LR and microcystin-RR. *Environ. Sci. Technol.* **2013**, *47*, 14376−14384.
(29) Le Manach, S.; Khenfech, N.; Huet, H.; Qiao, Q.; Duval, C.; Marie, A.; Bolbach, G.; Clodic, G.; Djediat, C.; Bernard, C.; Edery, M.; Marie, B. Gender-specific toxicological effects of chronic exposure to pure microcystin-LR or complex *Microcystis aeruginosa* extracts on adult medaka fish. *Environ. Sci. Technol.* **2016**, *50*, 8324−8334.
(30) Qiao, Q.; Le Manach, S.; Huet, H.; Duvernois-Berthet, E.; Chaouch, S.; Duval, C.; Sotton, B.; Ponger, L.; Marie, A.; Mathéron, L.; Lennon, S.; Bolbach, G.; Djediat, C.; Bernard, C.; Edery, M.; Marie, B. An integrated omic analysis of hepatic alteration in medaka fish chronically exposed to cyanotoxins with possible mechanisms of reproductive toxicity. *Environ. Pollut.* **2016**, *216*, 119−131.
(31) Garcia, G. R.; Noyes, P. D.; Tanguay, R. L. Advancements in zebrafish applications for 21st century toxicology. *Pharmacol. Ther.* **2016**, *161*, 11−21.
(32) Hou, J.; Li, L.; Wu, N.; Su, Y. J.; Lin, W.; Li, G. Y.; Gu, Z. M. Reproduction impairment and endocrine disruption in female zebrafish after long-term exposure to MC-LR: A life cycle assessment. *Environ. Pollut.* **2016**, *208*, 477−485.
(33) Liu, W. J.; Chen, C. Y.; Chen, L.; Wang, L.; Li, J.; Chen, Y. Y.; Jin, J. N.; Kawan, A.; Zhang, X. Z. Sex-dependent effects of microcystin-LR on hypothalamicpituitary-gonad axis and gameto-genesis of adult zebrafish. *Sci. Rep.* **2016**, *6*, 22819.
(34) Chen, L.; Zhang, X. Z.; Zhou, W. S.; Qiao, Q.; Liang, H. L.; Li, G. Y.; Wang, J. H.; Cai, F. The interactive effects of cytoskeleton disruption and mitochondria dysfunction lead to reproductive toxicity induced by microcystin-LR. *PLoS One* **2013**, *8* (1), e53949.
(35) Fu, J.; Han, J.; Zhou, B. S.; Gong, Z. Y.; Santos, E. M.; Huo, X. J.; Zheng, W. L.; Liu, H. L.; Yu, H. X.; Liu, C. S. Toxicogenomic responses of zebrafish embryos/larvae to tris(1,3-dichloro-2-propyl) phosphate (TDCPP) reveal possible molecular mechanisms of developmental toxicity. *Environ. Sci. Technol.* **2013**, *47*, 10574−10582.
(36) Lyu, K.; Meng, Q. G.; Zhu, X. X.; Dai, D. X.; Zhang, L.; Huang, Y.; Yang, Y. Changes in iTRAQ-based proteomic profiling of the Cladoceran *Daphnia magna* exposed to microcystin-producing and microcystin-free *Microcystis aeruginosa*. *Environ. Sci. Technol.* **2016**, *50*, 4798−4807.
(37) Feng, J. H.; Liu, H. L.; Bhakoo, K. K.; Lu, L. H.; Chen, Z. A metabonomic analysis of organ specific response to USPIO administration. *Biomaterials* **2011**, *32*, 6558−6569.
(38) Chen, L.; Zhang, X.; Chen, J.; Zhang, X. Z.; Fan, H. H.; Li, S. C.; Xie, P. NF-κB plays a key role in microcystin-RR-induced HeLa cell proliferation and apoptosis. *Toxicon* **2014**, *87*, 120−130.
(39) Huang, X.; Chen, L.; Liu, W. J.; Qiao, Q.; Wu, K.; Wen, J.; Huang, C. H.; Tang, R.; Zhang, X. Z. Involvement of oxidative stress and cytoskeletal disruption in microcystin-induced apoptosis in CIK cells. *Aquat. Toxicol.* **2015**, *165*, 41−50.
(40) Jiang, J. L.; Gu, X. Y.; Song, R.; Zhang, Q.; Geng, J. J.; Wang, X. R.; Yang, L. Y. Time-dependent oxidative stress and histopathological changes in *Cyprinus carpio* L. exposed to microcystin-LR. *Ecotoxicology* **2011**, *20*, 1000−1009.

DOI: 10.1021/acs.est.6b03990
Environ. Sci. Technol. 2017, 51, 596−607

(41) Roesner, A.; Hankeln, T.; Burmester, T. Hypoxia induces a complex response of globin expression in zebrafish (Danio rerio). *J. Exp. Biol.* **2006**, *209*, 2129−2137.
(42) Lam, S. H.; Winata, C. L.; Tong, Y.; Korzh, S.; Lim, W. S.; Korzh, V.; Spitsbergen, J.; Mathavan, S.; Miller, L. D.; Liu, E. T.; Gong, Z. Y. Transcriptome kinetics of arsenic-induced adaptive response in zebrafish liver. *Physiol. Genomics* **2006**, *27*, 351−361.
(43) Jacquemin, G.; Margiotta, D.; Kasahara, A.; Bassoy, E. Y.; Walch, M.; Thiery, J.; Lieberman, J.; Martinvalet, D. Granzyme B-induced mitochondrial ROS are required for apoptosis. *Cell Death Differ.* **2015**, *22*, 862−874.
(44) Wang, M. H.; Wang, D. Z.; Lin, L.; Hong, H. S. Protein profiles in zebrafish (Danio rerio) brains exposed to chronic microcystin-LR. *Chemosphere* **2010**, *81*, 716−724.
(45) Brown, K. H. Fish mitochondrial genomics: sequence, inheritance and functional variation. *J. Fish Biol.* **2008**, *72*, 355−374.
(46) Zhao, Y. Y.; Xie, P.; Fan, H. H.; Zhao, S. J. Impairment of the mitochondrial oxidative phosphorylation system and oxidative stress in liver of crucian carp (*Carassius auratus L.*) exposed to microcystins. *Environ. Toxicol.* **2014**, *29*, 30−39.
(47) Samuelsson, L. M.; Björlenius, B.; Förlin, L.; Larsson, D. G. J. Reproducible ^{1}H NMR-based metabolomic responses in fish exposed to different sewage effluents in two separate studies. *Environ. Sci. Technol.* **2011**, *45*, 1703−1710.
(48) He, J.; Li, G. Y.; Chen, J.; Lin, J.; Zeng, C.; Chen, J.; Deng, J. L.; Xie, P. Prolonged exposure to low-dose microcystin induces nonalcoholic steatohepatitis in mice: a systems toxicology study. *Arch. Toxicol.* **2016**, DOI: 10.1007/s00204-016-1681-3.
(49) Zhang, Z. Y.; Zhang, X.-X.; Wu, B.; Yin, J. B.; Yu, Y. J.; Yang, L. Y. Comprehensive insights into microcystin-LR effects on hepatic lipid metabolism using cross-omics technologies. *J. Hazard. Mater.* **2016**, *315*, 126−134.
(50) Thakur, P. C.; Stuckenholz, C.; Rivera, M. R.; Davison, J. M.; Yao, J. K.; Amsterdam, A.; Sadler, K. C.; Bahary, N. Lack of *de novo* phosphatidylinositol synthesis leads to endoplasmic reticulum stress and hepatic steatosis in cdipt-deficient zebrafish. *Hepatology* **2011**, *54*, 452−462.
(51) Qin, W. D.; Zhang, X. X.; Yang, L. Y.; Xu, L. Z.; Zhang, Z. Y.; Wu, J.; Wang, Y. P. Microcystin-LR altered mRNA and protein expression of endoplasmic reticulum stress signaling molecules related to hepatic lipid metabolism abnormalities in mice. *Environ. Toxicol. Pharmacol.* **2015**, *40*, 114−121.
(52) Ding, W. X.; Ong, C. N. Role of oxidative stress and mitochondrial changes in cyanobacteria-induced apoptosis and hepatotoxicity. *FEMS Microbiol. Lett.* **2003**, *220*, 1−7.
(53) Campos, A.; Vasconcelos, V. Molecular mechanisms of microcystin toxicity in animal cells. *Int. J. Mol. Sci.* **2010**, *11*, 268−287.
(54) Chen, L.; Xie, P. Mechanisms of microcystin-induced cytotoxicity and apoptosis. *Mini-Rev. Med. Chem.* **2016**, *16*, 1018−1031.
(55) Schönbrunner, E. R.; Schmid, F. X. Peptidyl-prolyl cis-trans isomerase improves the efficiency of protein disulfide isomerase as a catalyst of protein folding. *Proc. Natl. Acad. Sci. U. S. A.* **1992**, *89*, 4510−4513.
(56) Faltermann, S.; Grundler, V.; Gademann, K.; Pernthaler, J.; Fent, K. Comparative effects of nodularin and microcystin-LR in zebrafish: 2.Uptake and molecular effects in eleuthero-embryos and adult liverwith focus on endoplasmic reticulum stress. *Aquat. Toxicol.* **2016**, *171*, 77−87.
(57) Qin, W. D.; Xu, L. Z.; Zhang, X. X.; Wang, Y. P.; Meng, X. Y.; Miao, A. J.; Yang, L. Y. Endoplasmic reticulum stress in murine liver and kidney exposed to microcystin-LR. *Toxicon* **2010**, *56*, 1334−1341.
(58) Menezes, C.; Alverca, E.; Dias, E.; Sam-Bento, F.; Pereira, P. Involvement of endoplasmic reticulum and autophagy in microcystin-LR toxicity in Vero-E6 and HepG2 cell lines. *Toxicol. In Vitro* **2013**, *27*, 138−148.
(59) Christen, V.; Meili, N.; Fent, K. Microcystin-LR induces endoplasmatic reticulum stress and leads to induction of NFκB, interferon-alpha, and tumor necrosis factor-alpha. *Environ. Sci. Technol.* **2013**, *47*, 3378−3385.
(60) Van Scoy, A. R.; Lin, Y. C.; Anderson, B. S.; Philips, B. M.; Martin, M. J.; McCall, J.; Todd, C. R.; Crane, D.; Sowby, M. L.; Viant, M. R.; Tjeerdema, R. S. Metabolic responses produced by crude versus dispersed oil in Chinook salmon pre-smolts via NMR-based metabolomics. *Ecotoxicol. Environ. Saf.* **2010**, *73*, 710−717.
(61) Lu, S. C. S-Adenosylmethionine. *Int. J. Biochem. Cell Biol.* **2000**, *32*, 391−395.
(62) He, J.; Chen, J.; Wu, L. Y.; Li, G. Y.; Xie, P. Metabolic response to oral microcystin-LR exposure in the rat by NMR-based metabonomic study. *J. Proteome Res.* **2012**, *11*, 5934−5946.
(63) Zhao, S. J.; Xie, P.; Chen, J.; Liu, L. Y.; Fan, H. H. A proteomic study on liver impairment in rat pups induced by maternal microcystin-LR exposure. *Environ. Pollut.* **2016**, *212*, 197−207.
(64) Guo, X. C.; Chen, L.; Chen, J.; Xie, P.; Li, S. C.; He, J.; Li, W.; Fan, H. H.; Yu, D. Z.; Zeng, C. Quantitatively evaluating detoxification of the hepatotoxic microcystin-LR through the glutathione (GSH) pathway in SD rats. *Environ. Sci. Pollut. Res.* **2015**, *22*, 19273−19284.
(65) Marie, B.; Huet, H.; Marie, A.; Djediat, C.; Puiseux-Dao, S.; Catherine, A.; Trinchet, I.; Edery, M. Effects of a toxic cyanobacterial bloom (*Planktothrix agardhii*) on fish: insights from histopathological and quantitative proteomic assessments following the oral exposure of medaka fish (*Oryzias latipes*). *Aquat. Toxicol.* **2012**, *114*−*115*, 39−48.
(66) MacKintosh, C.; Beattie, K. A.; Klumpp, S.; Cohen, P.; Codd, G. A. Cyanobacterial microcystin-LR is a potent and specific inhibitor of protein phosphatases 1 and 2A from both mammals and higher plants. *FEBS Lett.* **1990**, *264*, 187−192.
(67) Honkanen, R. E.; Zwiller, J.; Moore, R. E.; Daily, S. L.; Khatra, B. S.; Dukelow, M.; Boynton, A. L. Characterization of microcystin-LR, a potent inhibitor of type 1 and type 2A protein phosphatases. *J. Biol. Chem.* **1990**, *265*, 19401−19404.
(68) Li, G. Y.; Chen, J.; Xie, P.; Jiang, Y.; Wu, L. Y.; Zhang, X. Z. Protein expression profiling in the zebrafish (*Danio rerio*) embryos exposed to the microcystin-LR. *Proteomics* **2011**, *11*, 2003−2018.
(69) Obri, A.; Ouararhni, K.; Papin, C.; Diebold, M. L.; Padmanabhan, K.; Marek, M.; Stoll, I.; Roy, L.; Reilly, P. T.; Mak, T. W.; Dimitrov, S.; Romier, C.; Hamiche, A. ANP32E is a histone chaperone that removes H2A.Z from chromatin. *Nature* **2014**, *505*, 648−653.
(70) Grunstein, M. Histone acetylation in chromatin structure and transcription. *Nature* **1997**, *389*, 349−352.10.1038/38664
(71) Jack, A. P. M.; Hake, S. B. Getting down to the core of histone modifications. *Chromosoma* **2014**, *123*, 355−371.

DOI: 10.1021/acs.est.6b03990
Environ. Sci. Technol. 2017, 51, 596−607

Supporting Information

Responses of the proteome and metabolome in livers of zebrafish exposed chronically to environmentally relevant concentrations of microcystin-LR

Liang Chen[†,‡,#], Yufei Hu[†,‡,#], Jun He[†], Jun Chen[†,*], John P. Giesy[§,∥,⊥], Ping Xie[†,*]

† Donghu Experimental Station of Lake Ecosystems, State Key Laboratory of Freshwater Ecology and Biotechnology, Institute of Hydrobiology, Chinese Academy of Sciences, Wuhan, 430072, China

‡ University of Chinese Academy of Sciences, Beijing, 100049, China

§ Department of Veterinary Biomedical Sciences and Toxicology Centre, University of Saskatchewan, Saskatoon, Saskatchewan S7N 5B3, Canada

∥ School of Biological Sciences, University of Hong Kong, Hong Kong SAR, China

⊥ State Key Laboratory of Pollution Control and Resource Reuse, School of the Environment, Nanjing University, Nanjing, 210089, China

 # These authors contributed equally to this work.

* **Authors for correspondence:** Jun Chen (Dr.), E-mail: chenjun@ihb.ac.cn, Ping Xie (Dr.), E-mail: xieping@ihb.ac.cn, Tel./Fax: +86-27-68780622, Institute of Hydrobiology, Chinese Academy of Sciences, No. 7 Donghu South Road, Wuhan, 430072, China

17 pages, 4 figures, 3 tables

Summary

iTRAQ-based quantitative proteomic analysis

Extraction of Proteins

Samples of liver were ground while frozen in liquid nitrogen, then powdered cells were transferred to 5 mL centrifuge tubes and sonicated three times on ice using a high intensity ultrasonic processor (Scientz) in lysis buffer (8 M urea, 1% Triton-100, 10 mM dithiothreitol (DTT, Sigma) and 0.1% Protease Inhibitor CocktailIV). The remaining debris was removed by centrifugation at 20,000g at 4 °C for 10 min. Finally, the protein was precipitated with cold 15% trichloroacetic acid (TCA) for 2 h at -20 °C. After centrifugation at 4 °C for 10 min, the supernatant was discarded. The remaining precipitate was washed with cold acetone for three times. The protein was redissolved in buffer (8 M urea, 100 mM TEAB, pH 8.0) and quantified by use of the 2-D Quant kit (GE Healthcare, Pittsburgh, PA) according to instructions provided by the manufacturer.

Digestion by Trypsin

For digestion, protein was reduced with 10 mM DTT for 1 h at 37 °C and alkylated with 20 mM iodoacetamide (IAA, Sigma) for 45 min at room temperature in darkness. For digestion with trypsin protein was diluted by adding 100 mM TEAB to a concentration of urea less than 2 M. Sequencing Grade Modified Trypsin (Promega) was then added at 1:50 trypsin-to-protein mass ratio for the first digestion overnight and 1:100 trypsin-to-protein mass ratio for a second digestion for 4 h. Approximately 100 μg protein for each sample was digested with trypsin for the following experiments.

iTRAQ Labeling

After digestion of proteins by trypsin, peptides were desalted by use of a Strata X C18 SPE column (Phenomenex) and vacuum-dried. Peptides were reconstituted in 0.5 M TEAB and processed according to the manufacturer’s protocol for 8-plex iTRAQ kit (AB Sciex, Foster City, CA). Briefly, one unit of iTRAQ reagent (defined as the amount of reagent required to label 50 μg of peptide) was thawed and reconstituted in

24 μl acetonitrile (ACN, Fisher Chemical). Mixtures of peptides were then incubated for 2 h at room temperature and pooled, desalted and dried by vacuum centrifugation.

Fractionation by HPLC

Samples were then fractionated by use of high pH, reverse-phase high-performance liquid chromatography (HPLC) using Agilent 300Extend C18 column (5 μm particles, 4.6 mm ID, 250 mm length, Santa Clara, CA). Briefly, peptides were first separated with a gradient of 2% to 60% acetonitrile in 10 mM ammonium bicarbonate pH 10 over 80 min into 80 fractions, Peptides were then combined into 18 fractions and dried by vacuum centrifuging.

LC-MS/MS Analysis

Peptides were dissolved in 0.1% formic acid (FA, Fluka), directly loaded onto a reversed-phase pre-column (Acclaim PepMap 100, Thermo Scientific). Separation of peptides was performed using a reversed-phase analytical column (Acclaim PepMap RSLC, Thermo Scientific). The gradient was comprised of an increase from 6% to 22% solvent B (0.1% FA in 98% ACN) over 26 min, 22% to 35% in 8 min and climbing to 80% in 3 min then holding at 80% for the last 3 min, all at a constant flow rate of 300 nl/min on an EASY-nLC 1000 UPLC system, The resulting peptides were analyzed by Q Exactive^{TM} Plus hybrid quadrupole-Orbitrap mass spectrometer (ThermoFisher Scientific, Waltham, MA).

Peptides were subjected to NSI source followed by tandem mass spectrometry (MS/MS) in Q Exactive^{TM} Plus (Thermo) coupled online to the ultra performance liquid chromatography (UPLC). Intact peptides were detected in the Orbitrap at a resolution of 70,000. Peptides were selected for MS/MS using NCE setting as 30; ion fragments were detected in the Orbitrap at a resolution of 17,500. A data-dependent procedure that alternated between one MS scan followed by 20 MS/MS scans was applied for the top 20 precursor ions with abundances greater than an ion count of 10,000 in the MS survey scan with 30.0s dynamic exclusion. The electrospray voltage applied was 2.0 kV. Automatic gain control (AGC) was used to prevent overfilling of

the ion trap; 50,000 ions were accumulated for generation of MS/MS spectra. For MS scans, the m/z scan range was 350 to 1800. Fixed first mass was set as 100 m/z.

Search of Database

The resulting MS/MS data were processed using Mascot search engine (v.2.3.0). Tandem mass spectra were searched against *Uniprot_zebrafish* database (41,054 sequences). Trypsin/P was specified as cleavage enzyme allowing up to 2 missing cleavages. Mass error was set to 10 ppm for precursor ions and 0.02 Da for fragment ions. Carbamidomethyl on Cys, iTRAQ-8plex (N-term) and iTRAQ-8plex (K) were specified as fixed modification and iTRAQ-8plex (Y), oxidation on Met was specified as variable modifications. False discovery rate (FDR) was adjusted to < 1% and peptide ion score was set ≥ 20 to reduce the probability of false peptide identification.

HR-MAS ^{1}H NMR-based metabolomic analysis

Sample preparation and ^{1}H NMR spectroscopy

Each sample of liver was rinsed in saline D_2O at 4 °C to maintain osmolality and to provide a field-lock, and placed into a 4 mm-diameter zirconium oxide (ZrO2) rotor with a spherical insert and a Kel-F cap. The total preparation time for each sample was less than 5 min. All high resolution magic-angle-spinning (HR-MAS) ^{1}H NMR spectra were recorded on a Bruke Avance 600 NMR spectrometer (Bruker Biospin, Germany) equipped with a triple-field resonance (^{1}H/^{13}C/^{31}P) high-resolution MAS probe, operating at a ^{1}H frequency of 600.13 MHz. Samples of tissue were spun at 5 KHz at the "magic-angle" (54.7°) and maintained at 283 K to minimize temperature-dependent metabolic changes. The one-dimensional Carr-Purcell-Meiboom-Gill (CPMG) spin-echo pulse sequence (recycle delay -90°-(τ-180°-τ)$_n$-acquisition) with a fixed total spin-spin relaxation delay, 2 nτ of 64 ms, was applied to acquire ^{1}H MAS NMR spectra of all samples. Water signals were pre-saturated by weak continuous wave irradiation on water resonance during the recycle delay. Typically, 64 transients were acquired with 32 K data points for each spectrum with a spectral width of 12.012 kHz, and the 90° pulse length was adjusted to approximately 9.5 μs for 90° pulse calibration individually for each sample. For assignment purpose, a series of 2D NMR spectra were acquired for some selected samples, including ^{1}H-^{1}H correlation spectroscopy (COSY), ^{1}H-^{1}H total correlation spectroscopy (TOCSY), ^{1}H J-resolved spectroscopy (JRES), ^{1}H-^{13}C heteronuclear single quantum correlation spectroscopy (HSQC), and ^{1}H-^{13}C heteronuclear multiple bond correlation spectroscopy (HMBC).

Processing of NMR Spectra

NMR spectra were processed by use of MestReNova (version 7.0, Mestrelab Research, Spain) and all free induction decays (FIDs) were multiplied by use of an exponential weighting function with a 0.3-Hz line broadening factor prior to Fourier transformation. Resulting NMR spectra were manually phased and baseline-corrected, then referenced to the internal lactate CH_3 resonance at 1.33 ppm. The spectral region

9.5-0.5 ppm was automatically divided into integral segments of equal width (0.004 ppm) and the regions of 6.08-5.45 ppm and 5.22-4.68 ppm (water) were removed.

Pattern Recognition Analysis and Statistics

For multivariate statistical analyses, after normalization of the spectra to the total integration value for each spectrum data from NMR spectra were imported to SIMCA-P+ (V11.0, Umetrics, Umea, Sweden). Principal component analyses (PCA) were performed by using a unit variance (UV) scaling approach, and the data were visualized in the form of PC score plots, in which each point represented an individual sample. A more sophisticated discriminant technique, partial least squares discriminant analysis (PLS-DA), was further applied to achieve global profile separation between the different treatments through maximizing systematic variance. Qualities of models were evaluated by 6-fold cross-validation parameters: R^2, indicating the total explained variation for the NMR data, and Q^2, indicating the predictability of the model, and an additional validation method, permutation test (permutation number = 200) was also conducted. Finally, the orthogonal projection to latent structure with discriminant analysis (OPLS-DA) method was utilized to identify the differential metabolites responsible for MC-LR exposure on unit variance scaled data. Coefficient plots provide information on spectral regions responsible for classification of samples and the significance of such contribution. Loadings in coefficient plots were calculated back from coefficients incorporating weights of variables contributing to the sample classification in the model. Coefficient plots were generated by use of MATLAB scripts (http://www.mathworks.com) with some in-house modifications and were color-coded with absolute value of coefficients (r). Correlation coefficients ($|r|$) > 0.755, which was determined according to the test for the significance of the Pearson's product-moment correlation coefficient, were considered statistically significant based on the discrimination significance at the level of $p < 0.05$ and degrees of freedom = 5.

Table S1. Quantitative real-time PCR (qRT-PCR) primer sequences for selected genes

Gene name	Abbreviation	Primer Sequence (5'-3')		Accession number	Product length (bp)
		Forward	Reverse		
phosphofructokinase, liver b	pfklb	GGATTTGAGGCGTATGAAGGA	TGATGGTGGCAGGAATGAC	NM_001328389.1	97
pyruvate kinase, liver and RBC	pklr	AACACAGATGCTGGAGAGTATG	CTCTACAGGGAAGTGTCCTTTG	NM_201289.1	139
pyruvate dehydrogenase (lipoamide) alpha 1a	pdha1a	CTGGTTGGACCCTCTCCTATTA	TCAATGTGGCTGGGAGATTTAG	NM_213393.1	112
succinate dehydrogenase complex, subunit A, flavoprotein (Fp)	sdha	CTCTGAGACCGCCATGATTT	GATGACCTGTCCCTTGTAGTTG	AY391458.1	118
NADH dehydrogenase subunit 1	nd1	TTGATGCTCAACCTGATCCC	CCCTATCCAGTACTCGACCTAA	KM207051.1	97
cytochrome c oxidase subunit I	coxI	GACGCCTATGCACTCTGAAATA	GGCGGTAAAGGCTTCTCATAA	AY996924.1	102
ATP synthase 6, mitochondrial	atp6	CCTTATCCTCGTTGCCATACTT	GTTTGTGAATCGTCCAGTCAATC	KT624627.1	115
protein disulfide isomerase family A, member 3	pdia3	GAGTTCTCTCGTGATGGAAAGG	CAGGAACGGGCTCAGATTTA	NM_001199737.1	94
peptidyl-prolyl cis-trans isomerase A-like	ppctia	CACTGACTGTGGAGAACTCAAG	ACCCAGAGCGTTCACATTATC	NM_001327972.1	101
endoplasmic reticulum to nucleus signaling 1, zebrafish homolog of human IRE1	ern1	ATGGGTAAGAAGCAGGATGTG	CAGGGACGAAGATGGACATAAC	NM_001020530.1	108
X-box binding protein 1, alternatively spliced	xbp1-1s	GATCCACTTCGACCACATCTAC	GACGGAATCCTCAGCTTTAACT	AY237651.1	88
eukaryotic translation initiation factor 2-alpha kinase 3, zebrafish homolog of human PERK	eif2ak3	GCCTCAGCAAACCAGAGATT	CTGAAGGAAACAGCCTCCATAC	BC122104.1	109
eukaryotic translation initiation factor 2, subunit 1 alpha a, zebrafish homolog of human eIF2α	eif2s1a	TTGATTGCTCCTCCTCGATATG	GCCTCTCTTCTCTTCGATCTTC	NM_199569.1	117
activating transcription factor 6	atf6	AAACCTCCACCTGTCACTATTC	CATTGACTGAGGCGTCTGAA	NM_001110519.1	102
activating transcription factor 4	atf4	CACACTGAGGTTCCAGTTCTC	TCGCTAATGTTCTGCTCTTCTT	BC067714.1	104
heat shock protein 5, zebrafish homolog of human glucose regulated protein 78	hspa5	GTGAACGAAGCCGAGAGATT	CGATCTGGTTCTTCAGGGAATAG	NM_213058.1	106
heat shock protein 90, beta (grp94)	hsp90b1	AGGCCCTGAAGGAACAAATC	CATGTTTCCAGACCATCCATACT	NM_198210.2	101
DNA-damage-inducible transcript 3, zebrafish homolog of human CHOP	ddit3	CTTCTTGTGGAGAGCGTGAAA	CGGTGGGAGACATTCACTAAAC	NM_001082825.1	97
glyceraldehyde-3-phosphate dehydrogenase	gapdh	AACCGTGTATGTGACCTGATG	TTCAACCAGATGGGAGAATGG	NM_001115114.1	104
18S small subunit ribosomal RNA	18S rRNA	GAGACTCCGGCATGCTAAAT	CAGACCTGTTATTGCTCCATCT	FJ915075.1	108

Table S2 Number of altered proteins in liver of zebrafish exposed to MC-LR.

		1 μg/L MC-LR vs control	10 μg/L MC-LR vs control
up-regulated	annotated/total	9/12	22/44
down-regulated	annotated/total	11/25	17/37
de-regulated	annotated/total	20/37	39/81

Table S3. Differentially expressed proteins (with functional annotation) in liver of zebrafish exposed to MC-LR.

Protein accession	Protein description	MW [Da]	pI	AASC [%]	MP	Score	Fold change[a]		Function category
							1 μg/L	10 μg/L	
Amino acid metabolism									
F1Q6E1	4-hydroxyphenylpyruvate dioxygenase	55878	6.21	48.2	18	1443	2.09±0.25	2.18±0.06*	tyrosine metabolism
Q6TGZ5	4-hydroxyphenylpyruvate dioxygenase	56913	6.33	50.9	19	1402	0.28±0.00**	0.30±0.02**	tyrosine metabolism
F1QHM8	Methylthioribulose-1-phosphate dehydratase	33409	6.1	12.9	2	73	0.98±0.03	0.73±0.03*	methionine metabolism
Q1RLT0	S-adenosylmethionine synthase	53891	6.38	12.8	3	55	1.02±0.02	0.72±0.01**	methionine metabolism
Protein metabolism									
A8E526	Rpl14 protein	23533	10.34	36.7	5	190	1.52±0.15	1.28±0.04*	ribosome biogenesis and assembly; protein biosynthesis
P62084	40S ribosomal protein S7	29842	10.09	20.6	3	221	1.30±0.06	1.35±003*	ribosome biogenesis and assembly; protein biosynthesis
Q6P5L3	60S ribosomal protein L19	33344	11.46	8.7	1	124	1.85±0.40	1.44±0.03*	ribosome biogenesis and assembly; protein biosynthesis
Q6PBV6	H/ACA ribonucleoprotein complex subunit 2-like protein	23655	9	24.7	2	51	1.40±0.09*	1.12±0.07	ribosome biogenesis and assembly; protein biosynthesis
F1Q5S9	Probable signal peptidase complex subunit 2	30634	7.57	8.9	3	89	1.18±0.06	1.35±0.06*	protein processing
Q6NWJ2	Signal peptidase complex subunit 3 homolog (S. cerevisiae)	24556	8.63	19.4	3	100	1.32±0.14	1.45±0.06*	protein processing
Q7T2E1	SEC13 homolog (S. cerevisiae)	41561	5.04	18.8	3	230	1.14±0.11	1.39±0.09*	protein transport
Lipid metabolism									

A3QK15	Acetoacetyl-CoA synthetase	89178	6.15	14.9	8	124	1.61±0.66	0.69±0.03*	Fatty acid metabolism
Q4V8S5	Acbd7 protein	14575	7.85	48.9	2	128	1.95±0.19*	1.48±0.15	atty-acyl-CoA binding
Q58EG2	Erlin-1	46984	6.18	37.1	11	260	1.12±0.01	1.33±0.03*	lipid metabolism
Q6DRN8	Cdipt protein	26678	6.57	13.1	2	36	0.97±0.04	1.30±0.06*	lipid metabolism
Q7T2J4	Alcohol dehydrogenase 8b	51445	7.8	30.9	11	689	0.90±0.16	0.67±0.05*	lipid metabolism
Q9I8L5	Fatty acid-binding protein 10-A, liver basic	18977	8.87	51.6	5	2021	0.99±0.11	0.82±0.02*	Fatty acid transport
O42364	Apolipoprotein Eb	37491	4.88	6.4	1	35	0.89±0.13	0.72±0.01**	lipid transport; lipoprotein metabolism
Mitochondrial energy metabolism									
Q6AZA2	NADH dehydrogenase (Ubiquinone) flavoprotein 1	62421	8.72	16.3	5	165	0.89±0.03	0.69±0.03*	electron transport chain
Q6IQM2	Cytochrome c	16734	9.46	29.8	2	114	0.85±0.10	0.70±0.04*	electron transport chain
Q9MIY7	Cytochrome c oxidase subunit 2	27964	4.6	10.4	2	42	1.21±0.02*	1.05±0.07	electron transport chain
Other metabolism									
A2BHD8	Beta-hexosaminidase	71741	5.77	29.4	12	480	1.22±0.03*	1.38±0.16	beta-N-acetylhexosaminidase activity
F8W5B8	Phosphorylase	116134	6.09	46.8	28	1911	0.79±0.17	0.70±0.03*	glycogen phosphorylase activity
Q0E671	Cytidine monophosphate sialic acid synthetase 1	59775	7.59	6.7	2	103	1.33±0.07*	1.22±0.09	nucleotidyltransferase activity
Q5CZW2	Uridine phosphorylase	30974	5.47	29.6	3	100	0.75±0.08	0.76±0.03*	nucleotide metabolism
Q7ZUN6	Phosphoribosylaminoimidazole carboxylase, phosphoribosylaminoimidazole succinocarboxamide synthetase	57409	6.99	21.9	6	195	1.08±0.17	0.73±0.02**	nucleotide metabolism
Q8UVG6	Cellular retinol-binding protein type II	21443	6.09	16.3	3	39	0.74±0.15	0.54±0.02**	vitamin A metabolism
Chromatin assembly and modification									
E7F4R5	Histone deacetylase 8	178359	5.44	1.7	2	82	0.82±0.18	0.70±0.02*	histone deacetylase activity

G1K2S9	Histone H3	19721	11.27	5.1	1	42	1.34±0.11	1.59±0.12*	chromatin assembly
Q1RLR9	Histone H2A	47695	9.98	7.6	2	58	1.58±0.07*	1.68±0.23	chromatin assembly
Q6NUW5	Acidic leucine-rich nuclear phosphoprotein 32 family member E	32852	3.86	16	3	164	1.38±0.13	1.23±0.04*	H2A.Z chaperone
Signal transduction									
F1QT29	Calcium uniporter protein, mitochondrial	48911	9.15	5.9	2	79	0.82±0.03*	1.00±0.04	calcium uptake into mitochondria
Q1LWV8	Phosphoinositide phospholipase C	173688	5.69	2	2	55	0.82±0.03*	0.82±0.04	signal transducer activity
Q2L6L1	Protein canopy-1	27138	4.97	23.5	3	125	1.57±0.33	1.52±0.08*	fibroblast growth factor receptor signaling pathway
Q803G3	Serine/threonine-protein phosphatase	39760	5.21	28.8	6	186	0.82±0.01*	0.98±0.03	signal transduction
Immune response									
C1IHU8	Intelectin 1	40147	6.3	9.6	2	100	0.64±0.03**	0.58±0.02**	immune response
Q24JW2	Lysozyme	22596	8.79	15.2	2	69	0.39±0.08*	0.39±0.24	immune response
Q6PFU1	CD81 antigen	31180	5.79	12.3	2	47	0.62±0.04*	0.62±0.13	immune response
Q7ZVM6	Cytotoxic granule-associated RNA binding protein 1, like	44791	8.36	12	2	39	1.18±0.18	1.43±0.03*	immune response
Q6PHG2	Hemopexin	63485	6.14	21.5	9	255	0.58±0.11	0.50±0.05*	inflammatory response
Response to stress									
F1QUW4	Hypoxia up-regulated protein 1	142122	4.98	24.7	15	661	1.29±0.25	1.27±0.03*	response to hypoxia
Q90486	Hemoglobin subunit beta-1	19040	7.7	79.7	10	1929	0.62±0.04*	0.84±0.24	response to hypoxia
E9QH31	Aldehyde dehydrogenase	67706	8.82	19.8	8	164	1.21±0.03*	1.22±0.05	oxidoreductase activity
F1QUR3	Protein disulfide-isomerase (Fragment)	67626	6.76	42.5	16	1248	1.30±0.21	1.44±0.10*	protein folding
Q6NYZ0	Dnajb11 protein	49612	5.63	15.3	3	148	1.27±0.23	1.28±0.03**	protein folding
Q6PE26	Calr protein	63340	4.38	35.2	13	491	1.56±0.34	1.47±0.05**	protein folding
Q7ZZA3	Peptidyl-prolyl cis-trans isomerase	26598	7.68	19.8	3	82	1.50±0.11*	1.20±0.10	protein folding
Z4YIA7	Calumenin-A	46617	4.46	27.8	5	199	1.51±0.22	1.48±0.04*	protein folding

Other function									
Q7SXF6	Cysteine-rich with EGF-like domain protein 2	47349	4.6	6.7	2	35	1.40±0.40	1.39±0.03**	calcium ion binding
Q7ZT36	Parvalbumin 3	15248	4.43	50.5	5	100	0.74±0.03*	1.12±0.27	calcium ion binding
E9QB46	Selenium-binding protein 1	62051	5.93	21.6	5	279	1.34±0.09	1.44±0.04*	selenium binding
Q6DGU5	Solute carrier family 25 member 46	48930	8.42	11.4	2	51	0.81±0.01*	0.84±0.01	mitochondrial membrane fission; transport
F1QT89	Reticulon	27018	8.43	16.8	2	66	1.13±0.11	1.24±0.03*	membrane morphogenesis
Q5U3G0	Progesterone receptor membrane component 1	26524	4.75	20.7	3	150	1.35±0.12	1.62±0.07**	progesterone receptor
Q64HD0	Sex hormone binding globulin	50714	5.63	13.9	4	109	0.71±0.02*	0.79±0.08	sex hormone transport
F1QRA6	Tetratricopeptide repeat protein 38	60923	5.78	21.9	8	250	0.93±0.11	0.73±0.02*	unknown
Q8AW82	Novel protein similar to human proliferation-associated 2G4 protein (PA2G4)	57080	8.03	18.4	6	132	1.22±0.02*	1.03±0.03	growth regulation

[a] The fold changes are indicated as compared to the controls. Values >1 indicate up-regulation, and values < 1 indicate down-regulation. Proteins with fold difference > 1.2 or < 0.83 and $p < 0.05$ were considered significantly altered, which are indicated with * ($p < 0.05$) or ** ($p < 0.01$).

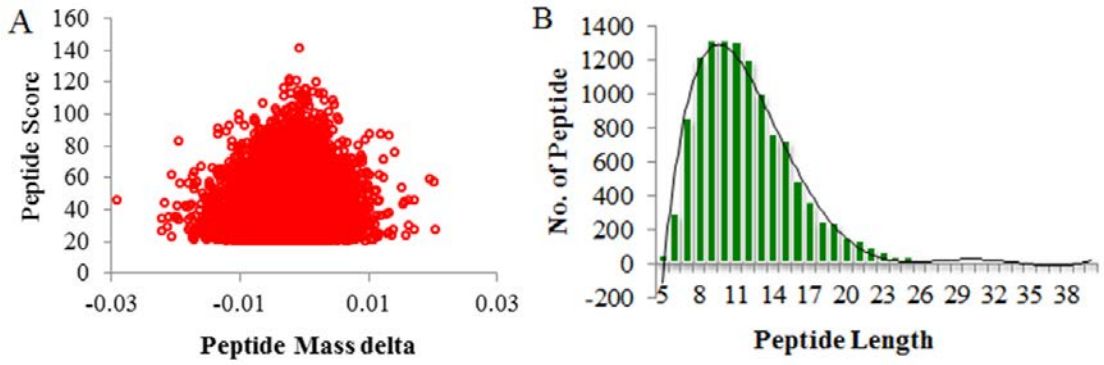

Figure S1. Quality control validation of mass spectrometry data (A) mass error distribution and (B) peptide lengths of peptides identified by iTRAQ.

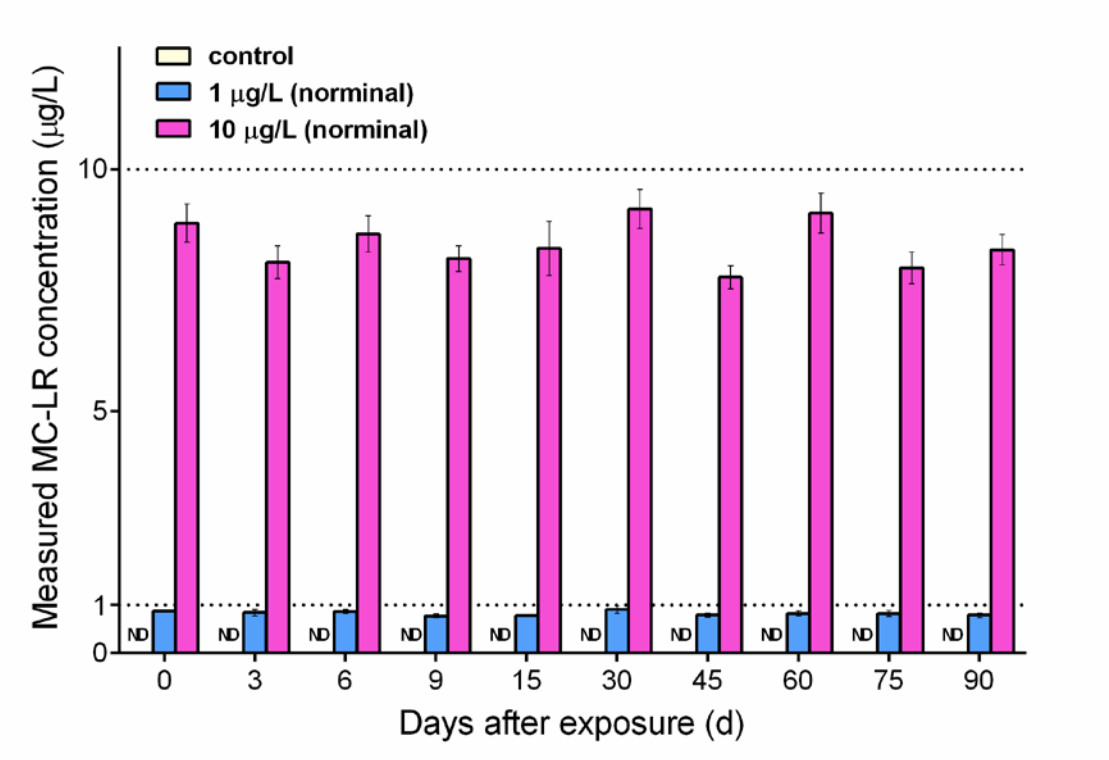

Figure S2. Concentrations of MC-LR measured in water during the 90-day study. Values are presented as the mean ± standard error (SE). ND, indicates not detected, i.e. lower than the minimum detection limit (MDL, 0.1 μg/L).

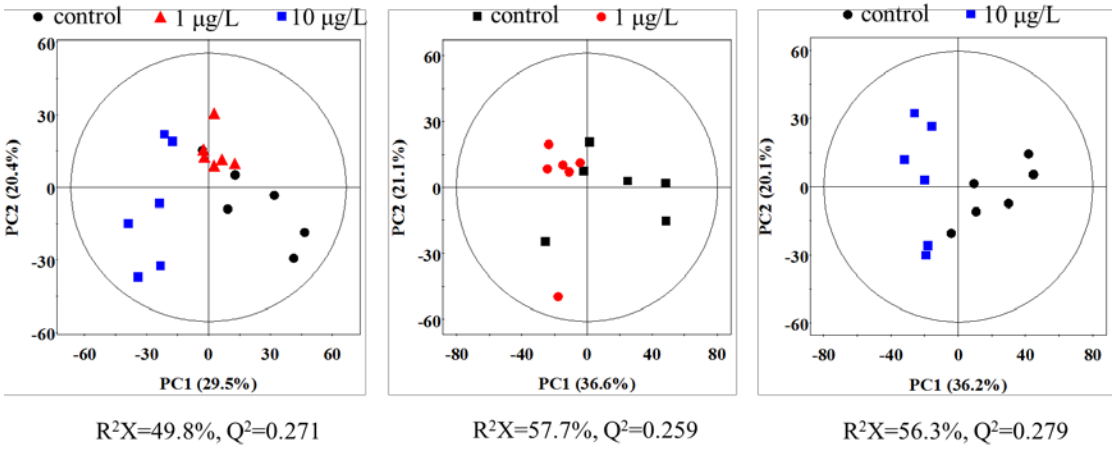

R^2X=49.8%, Q^2=0.271 R^2X=57.7%, Q^2=0.259 R^2X=56.3%, Q^2=0.279

Figure S3. PCA score plots based on ^{1}H HR-MAS CPMG NMR spectra of livers of zebrafish exposed to MC-LR.

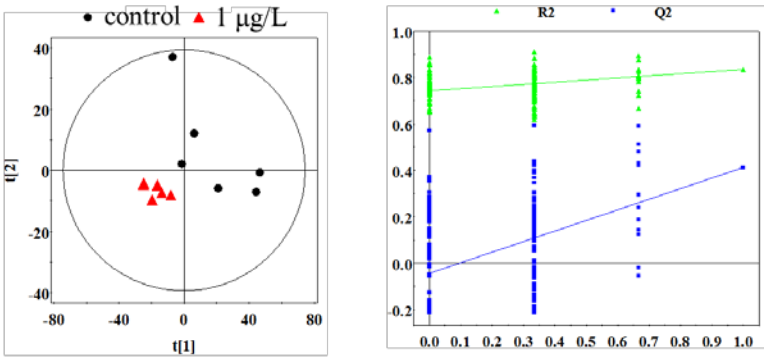

R^2X=45.5%, R^2Y=0.836, Q^2=0.414

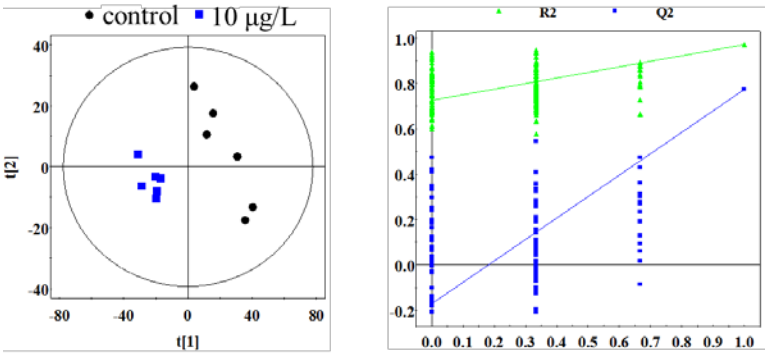

R^2X=46.0%, R^2Y=0.971, Q^2=0.774

Figure S4. PLS-DA score plots (left panel) derived from ^{1}H HR-MAS CPMG NMR spectra of livers of zebrafish exposed to MC-LR and cross validation (right panel) by permutation test (n=200).